NWC TP 7124

A Fragmentation Model for Cylindrical Warheads

by
John Pearson
Research Department

DECEMBER 1990

NAVAL WEAPONS CENTER
CHINA LAKE, CA 93555-6001

Naval Weapons Center

FOREWORD

This document reports work that was conducted as part of a continuing program in the study of both the natural fragmentation and the controlled fragmentation of warheads.

This work was performed during fiscal years 1990 and 1991. Funding for this effort was provided by the Office of Naval Research under Work Requests No. N0001490WX4E008 and N0001491WX4E009.

This report has been reviewed for technical accuracy by Stephen A. Finnegan.

Approved by
R. L. DERR, *Head*
Fuze and Sensors Department
11 December 1990

Under authority of
D. W. COOK
Capt., U.S. Navy
Commander

Released for publication by
W. B. PORTER
Technical Director

NWC Technical Publication 7124

Published by ..... Technical Information Department
Collation ..... Cover, 24 leaves
First printing ..... 260 copies

REPORT DOCUMENTATION PAGE

Form Approved
OMB No. 0704-0188

1. AGENCY USE ONLY *(Leave blank)*	2. REPORT DATE	3. REPORT TYPE AND DATES COVERED
	December 1990	Final; Dec 1989 - Nov 1990

4. TITLE AND SUBTITLE
A Fragmentation Model for Cylindrical Warheads

5. FUNDING NUMBERS
N0001490WX4E008
N0001491WX4E009

6. AUTHORS
John Pearson

7. PERFORMING ORGANIZATION NAME(S) AND ADDRESS(ES)
Naval Weapons Center
China Lake, CA 93555-6001

8. PERFORMING ORGANIZATION REPORT NUMBER
NWC TP 7124

9. SPONSORING/MONITORING AGENCY NAMES(S) AND ADDRESS(ES)

10. SPONSORING/MONITORING AGENCY REPORT NUMBER

11. SUPPLEMENTARY NOTES

12a. DISTRIBUTION /AVAILABILITY STATEMENT
Approved for public release; distribution is unlimited

12b. DISTRIBUTION CODE

13. ABSTRACT *(Maximum 200 words)*

This report presents a descriptive model for the expansion and fragmentation behavior for the case of a single-point, end-initiated cylindrical warhead. This model divides the overall behavioral process of the warhead case into four distinct zones of behavior which occur between initial case motion and fragment impact. The report describes what is happening in each zone in terms of (1) the physical behavior of the warhead case and (2) the respective velocities of the metal case or fragments. This model is based on the results of numerous experimental studies using high speed photography and fragmentation test arenas. Several examples in the use of the model are presented based on these studies.

14. SUBJECT TERMS
Fragmentation, warheads, fragment velocities, high-speed photography, Bridgman Effect

15. NUMBER OF PAGES
46

16. PRICE CODE

17. SECURITY CLASSIFICATION OF REPORT	18. SECURITY CLASSIFICATION OF THIS PAGE	19. SECURITY CLASSIFICATION OF ABSTRACT	20. LIMITATION OF ABSTRACT
UNCLASSIFIED	UNCLASSIFIED	UNCLASSIFIED	SAR

CONTENTS

INTRODUCTION

When a warhead detonates, the warhead case does not instantaneously turn into a family of well-defined, high-velocity fragments. Rather, there is a finite time, normally measured in microseconds to fractions of a millisecond, within which the warhead case undergoes a rather complicated behavioral process of "expansion — to fracture — to fragmentation," which results in the formation of the discrete fragments with which most ordnance engineers are familiar.

The major variables which govern this behavioral process appear to be the charge-to-mass ratio (C/M) of the warhead, the engineering properties of the case material, and the energetic characteristics of the explosive. For a more well-defined overview of the total system behavior which includes the spatial and temporal projection of fragments, the geometry of the initiation system, the length-to-diameter ratio (L/D) of the warhead, and the degree of end closure of the cylindrical case all need to be considered. These latter variables, however, relate more to the behavior of fragments after formation than to the initial behavior leading to their formation.

The intent of this report is to present a descriptive model for the expansion and fragmentation behavior for the case of a single-point, end initiated warhead. This model divides the cylinder expansion and fragmentation process into four distinct phases or zones in order to better understand what is happening in each zone in terms of (1) the case expansion to fragmentation behavior and (2) the respective velocities of the metal case or fragments; and to treat these phases or zones as a function of distance and time. While these four phases or zones are all tied together in a continuing model of behavior, certain features may occur in each which are not common to all. Identifiable physical events may be used to establish the start and the completion of each phase or zone.

While the terms "phase" and "zone" are used somewhat interchangeably in this report they do have specific meanings. The term "phase" actually refers to a behavioral mode in the expansion and fragmentation of the case. The term "zone" refers to a measurable distance for which a corresponding phase is operable. Thus, Zone 1 is the distance within which Phase 1 behavior of the warhead case occurs.

This first attempt by the author at defining such a spectrum of phases stresses the behavioral modes of the cylinder and how they are linked together. Within each phase of behavior are many finer details of interest. No attempt is made to get into such details in this report.

In addition to providing a behavioral treatment of the cylinder or warhead case from detonation to target impact, a discussion of the overall velocity behavior of the case is also presented. A review of earlier experimental and theoretical studies was made to see if it was practicable to use a series of four representative velocities, one for each zone of behavior. Such an approach would provide an engineering "rule of thumb," which would allow an ordnance investigator to establish both the behavioral condition of the warhead case and an approximate velocity of the case or fragments for each of the four zones of interest.

The behavioral mode and the velocity mode initially are treated separately. When the two treatments are combined later in the report the result is a fragmentation model which offers actual examples of the engineering "rule of thumb" approach mentioned above.

In the latter part of this report some other considerations are discussed which help to clarify the conditions which govern the physical behavior of the warhead case after the start of detonation and the resulting velocity of the fragments. This information, when interwoven into the behavior of the fragmentation model, helps to provide a more thorough understanding of the total case behavior of a fragmentation warhead.

In preparing this report the approach has been largely descriptive, based mainly on the experimental results of earlier studies by the author. These results have been complemented by additional data provided by the works of both recent and early-date investigators. In addition to providing a simplified way of viewing a very complex problem, it is also intended that this report should serve as a training guide or as an introduction to the subject for people entering the warhead field.

EXPERIMENTAL BASIS

The fragmentation model described in this report, and the representative values given in the examples, are based on the results of a number of separate studies conducted intermittently by the author over a period of years. The original studies each dealt with some specific aspect of warhead fragmentation such as temperature, engineering properties of the case material, explosive proper-

ties, fragmentation control parameters, multi-wall case design, fabrication techniques, and others.

Most of these studies were conducted using a standard size test vehicle; namely, an open ended steel cylinder 5-in. OD x 4 1/2-in. ID x 10-in. long. A variety of different steels and explosive types were used in these studies. However, for comparison purposes and for use as a standardized base, a standard test cylinder design was used which consisted of SAE 1015 steel for the case material, Comp C-3 as the explosive, and single-point end initiation for detonating the explosive. These studies were conducted primarily for post-mortem evaluation of the fragments and involved the use of standardized arenas for fragment recovery, spatial distribution, and fragment velocities. Fractographic and metallographic studies were also conducted on recovered fragment specimens. Details of many of these studies are given in References 1 through 4.

Companion studies frequently involved the use of a Cordin high speed framing camera in order to obtain an understanding of the early phase of the fragmentation process under various test conditions. For recording the early behavior of the test cylinder the Cordin camera was operated at 333,000 frames per second. At this framing rate the interframe time between pictures was 3 microseconds, with the interframe time being measured from peak to peak illumination between successive pictures in a sequence of 26 frames on 35-mm color film. Effective exposure time for recording the event for each frame was about 3/4 microsecond. Lighting for each event was provided by means of two tubular argon flash bombs located on either side, and slightly forward of the cylinders. Colored backboards set behind the test round were used to accent the expansion behavior of the cylinder.

At a framing rate of 333,000 frames per second the recording time for each test was about 75 microseconds. This was an excellent time period in which to view the overall process from the start of detonation until the fragmentation process was obscured by detonation products. However, to study the behavior of any specific location along the cylinder wall there is a shorter "viewing window" which starts when the passage of the detonation front within the cylinder starts to radially displace that section of the cylinder, and stops when the detonation products emanating from fractures in that location obscure any further detailed viewing of the event. With the cylinder dimensions previously given, and with single-point end initiation, the "viewing window" time for a location about half way down the cylinder was about 36 microseconds. More detailed information on these high-speed photographic studies is presented in Reference 5.

These early studies by the author used 5-in. OD cylinders since this is a typical size used in many U.S. Navy weapons. It is also a size (not too big, not too small) which readily allows for theoretical adjustment of behavioral patterns

to other size warheads. The use of plain, low-carbon steels was stressed in these studies since they are widely used for non-penetrating warheads. These steels have the advantages of low cost, excellent machinability, and when used with shear-control grids for controlled fragmentation warheads they have an excellent "forgiving nature" for minor discrepancies in the fabrication of the control grids. Also, for laboratory analysis they provide excellent fractographic and microstructural signatures of the event. For most of these earlier experimental studies the test cylinders had a C/M ratio in the range 0.85 to 0.90. For a detailed discussion of the shear-control method for controlling warhead fragmentation the reader is referred to Reference 4.

The plain, low-carbon steels behave in an extremely ductile manner when used as the case material for fragmentation warheads. With a C/M ratio of the size given above, the cylinder wall fractures completely in shear. For substantially smaller C/M ratios (more metal, less explosive), or for some of the higher strength, heat-treatable steels which demonstrate less ductility in the fragmentation process, it is possible to obtain case fractures which are a combination of shear fracture for the inner portion of the wall and tensile fracture for the outer portion of the wall (Reference 6).

The fragmentation model described in the next section is based on the expansion behavior of a ductile steel case which fractures completely in shear. For the combination type of fracture the fragmentation model described is appropriate in the general sense, but the descriptive appearance of fracture growth and its mode of expansion into the fragmentation process may require some modification.

BEHAVIORAL MODE

GENERAL

For ease of study or presentation, the behavioral mode of an explosively-loaded steel cylinder or warhead case can be divided into four distinct phases, with definite features which can be used to separate and identify the four phases. In discussing these phases it is easiest to look at the behavior of one cross-sectional slice of the warhead case. In the qualitative sense, each such section of the warhead case follows the same general model, except that the behavior of these sections is sequential in time and follows the propagation of the detonation front through the explosive. In the quantitative sense, some variations may occur between different axial locations in the warhead based on such factors as the L/D of the warhead and the possible introduction of end effects.

The descriptive aspects of the following four phases are based on the behavior of a cylinder machined from a plain, low-carbon steel such as SAE 1015 with an initial hardness of about R_B 78 to R_B 85, and an ultimate strength of about 65,000 to 70,000 psi. The details of early behavior are taken from Cordin camera records.

PHASE 1 — ELASTIC-PLASTIC EXPANSION

For a representative cross-sectional slice of the warhead case, Phase 1 starts when the detonation front passes this location in the warhead case and the case shows the first sign of radial expansion. This initial phase represents elastic-plastic expansion (mostly plastic) of the warhead case. During the expansion process of this phase the case remains complete without the visible presence of any fracture; that is, the cylinder expands to its limiting condition prior to the first sign of fracture.

This phase comes to an end when the first sign of fracture appears on the outer surface of the cylinder or case. These fractures first appear as hairline markings oriented in the axial direction. When viewed with a high-speed framing camera, a small number of these initial fractures will first appear in the same time frame and will be spaced roughly equidistant around the cylinder. As previously mentioned, a typical framing rate for this type of study might be 333,000 frames per second where one interframe time is 3 microseconds. In Phase 2 these initial hairline fractures become the major fractures in the continuous growth of a complex fracture system.

PHASE 2 — CONTINUING PLASTIC EXPANSION WITH OPENING FRACTURES

During Phase 2 the cylinder or case continues expanding in the plastic condition. At the same time, additional axially oriented fractures appear on the outside surface of the cylinder. All such fractures first appear as hairline markings, and then follow a growth pattern in which they both lengthen and open up, i.e., widen in the circumferential direction, as they extend inward toward the inner surface. During this growth phase the surface fractures take on the characteristic appearance of a relatively narrow ellipse with sharp ends. The center of the ellipse continuously widens during this phase.

Phase 2 ends for quantitative viewing purposes when the detonation products appear in the mouth of the fracture. At this time, the products within the mouth of the fracture appear as a smooth, dark surface not unlike the surface of a bubble, or a portion of a balloon just starting to protrude through an opening.

The major fractures have now propagated completely through the cylinder wall. The first fractures to show the presence of the detonation products are also the largest and most prominent fractures in the field of view. They also tend to be the same fractures whose appearance concluded the Phase 1 behavior.

PHASE 3 — THE FRAGMENTATION PROCESS WITHIN THE DETONATION PRODUCTS CLOUD

Warhead case behavior in Phase 3 is mostly obscured by the presence of the detonation products which emanated through the cylinder wall. A quantitative understanding of this process would require a study using flash radiographic techniques. However, even without such studies it is possible to describe the behavior in the qualitative sense.

The expansion process of Phase 2 continues into Phase 3. At this time, the velocity of the detonation products issuing from the fractures is greater than the radial velocity of the case so that obscuration develops rapidly and continuously increases into the form of an expanding cloud of detonation products which surrounds the warhead case.

Under the continuing expansion of the case each fracture continues to lengthen and widen but on a much greater scale than in Phase 2. This expanding fracture system undergoes a considerable amount of cross linkage which initially ties the major pieces together. At this time the fragment components are quite narrow compared to their lengths, and they may involve numerous instances of bifurcation which are involved in the cross linkage aspects of the expansion. The overall appearance may be somewhat like that of an expanding latticework oriented in the axial direction. The separation of these cross linkages produces a number of long, narrow, discrete fragments in the major portion of the warhead case. It is expected that the more ductile materials will show the above behavior the most. The more brittle materials should show less of this cross linkage effect, with the major fragments separating more quickly. End effects may already have produced smaller fragments at both ends of the cylinder.

Even after the formation of these long, narrow fragments the fragmentation process may still continue for some period of time, but in a different manner. As these long fragments are projected outward, the relative motions of the fragment elements which relate to relative axial particle velocities along the fragment length, tend to reduce the initially long fragment into a number of shorter pieces. This part of the fragmentation process can be substantially influenced by the geometry of the initiation system. A treatment of this latter topic is presented in Reference 7.

The expansion velocity of the products cloud begins to slow down while the metal velocities are maintained, so that at some point in time the fragments emerge from the cloud, thus completing Phase 3. It should be noted that at the end of Phase 3 the products cloud may still be expanding, but not fast enough to contain the fragments.

PHASE 4 — DISCRETE FRAGMENTS IN TERMINAL FLIGHT

This phase starts with the emergence of the fragments from the detonation products cloud and continues until the fragments engage the target, or come to rest by some other means — or it may be considered as ended merely when the fragments pass from the useful zone of consideration. There is some thought that the final phase of the fragmentation process, that part in which major fragments are being reduced to several shorter pieces in the axial direction, may still be taking place in the early part of Phase 4.

BEHAVIORAL SUMMARY

Figure 1 shows a series of four pictures taken from a Cordin camera sequence for a plain wall cylinder of SAE 1015 steel detonated at normal temperature. The pictures show the expanding cylinder at about 30, 36, 42, and 48 microseconds after the start of detonation. Pictures such as these, in complete 26 frame sequences, were the basis for establishing cylinder behavior during Phases 1 and 2 and the early behavior during the start of Phase 3. Other examples of high-speed photography, similar to Figure 1, which show the effects of inner surface shear-control grids and low temperatures, are presented in Reference 5.

The sketches of Figure 2 show the cross section of an expanding cylinder with the identifying features indicated for the start of each of the four phases. The model shown is for the behavior of a ductile steel cylinder which fractures completely in shear and matches the behavior of the cylinder shown in Figure 1. The sketches do not take into account any dimensional changes in the diameter and wall thickness of the cylinder which occur during the expansion process.

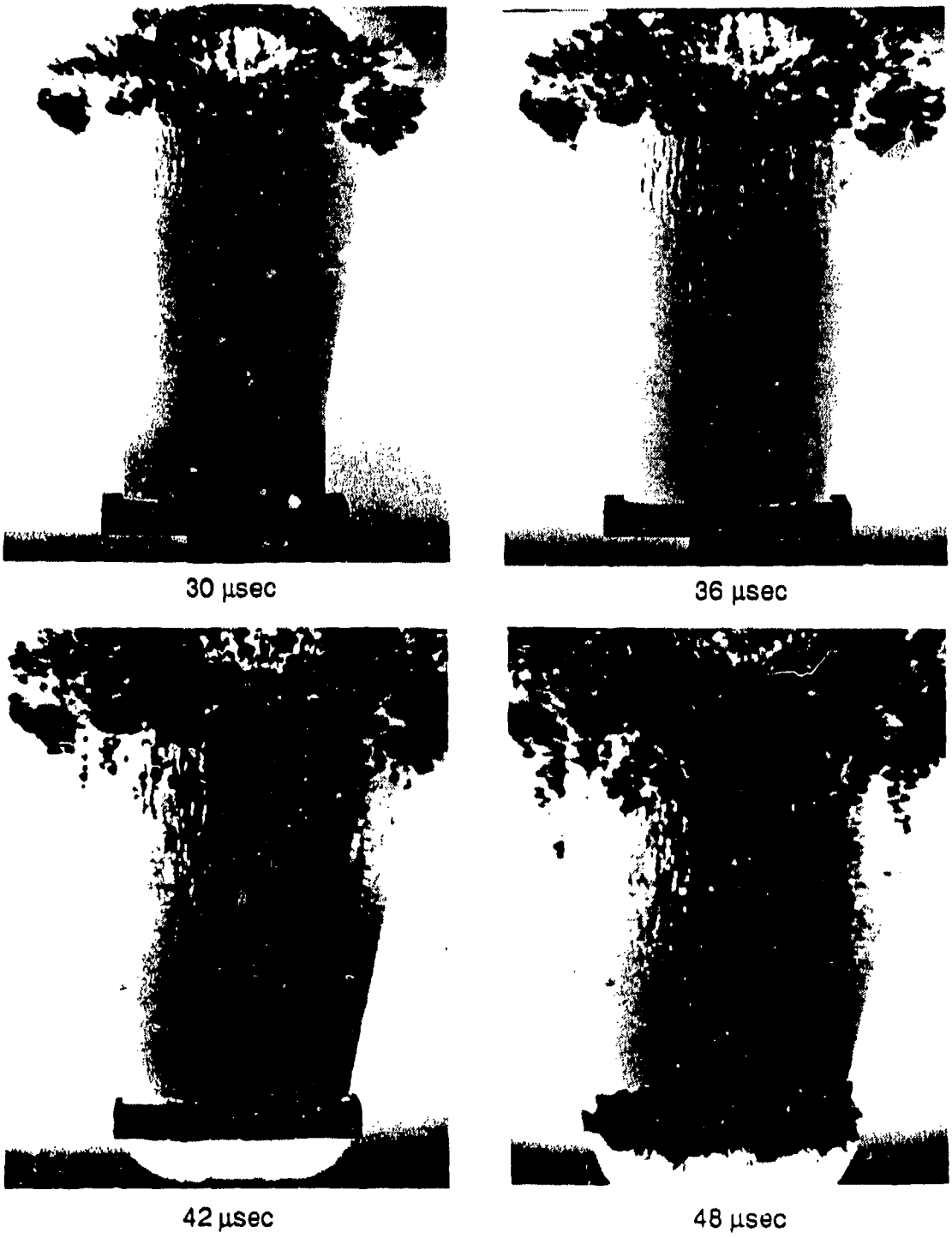

FIGURE 1. Behavior of Plain Wall Cylinder (+80°F) at About 30, 36, 42, and 48 Microseconds After the Start of Detonation.

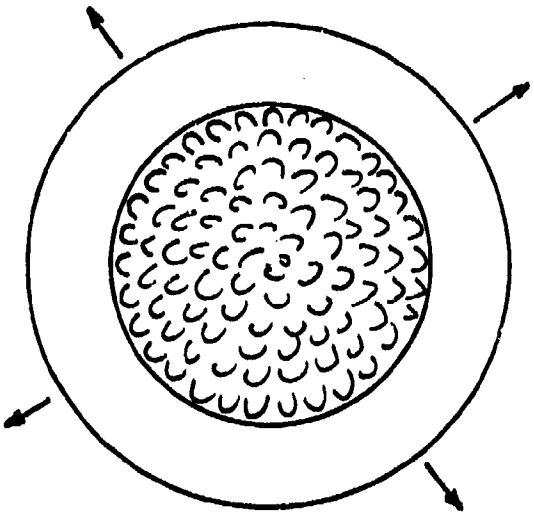

START OF PHASE I
RADIAL EXPANSION BEGINS

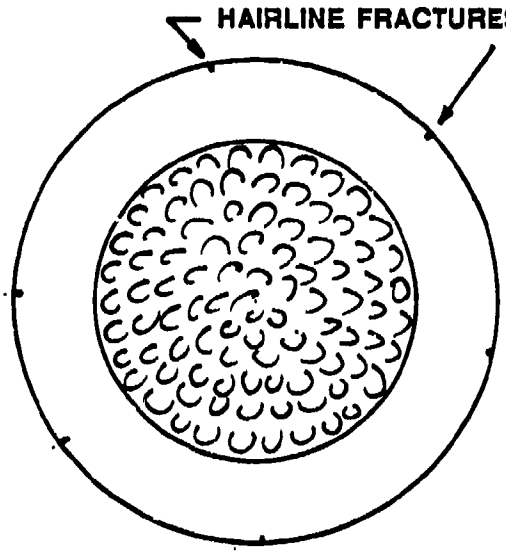

START OF PHASE 2
HAIRLINE FRACTURES FIRST
APPEAR ON OUTER SURFACE

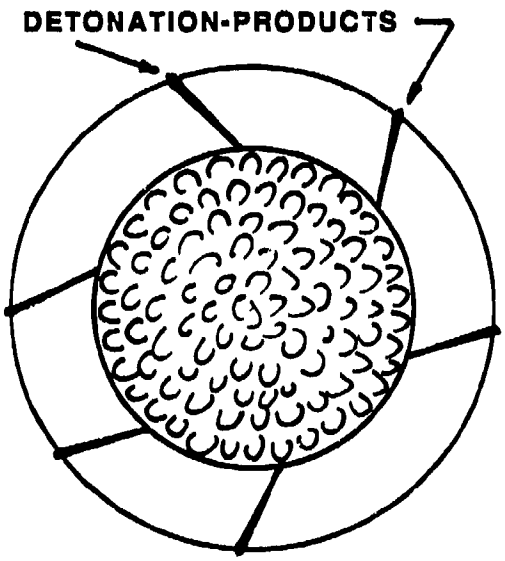

START OF PHASE 3
DETONATION PRODUCTS START
TO EMANATE FROM FRACTURES

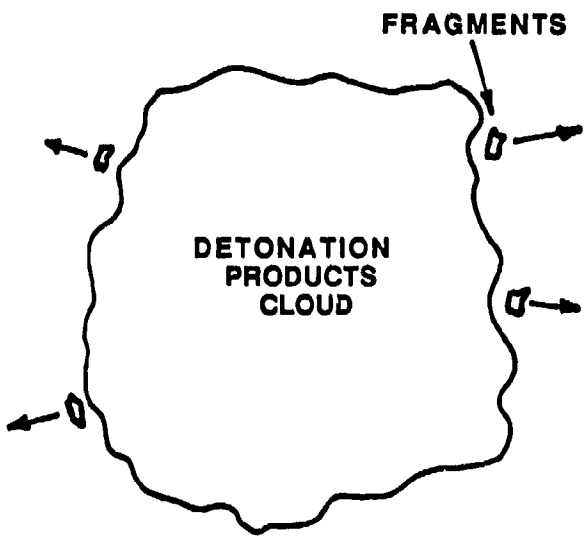

START OF PHASE 4
FRAGMENTS ISSUE FROM
DETONATION PRODUCTS CLOUD

FIGURE 2. Cross-Sectional Sketches of an Expanding Cylinder Which Identify the Start of Each of the Four Phases.

REPRESENTATIVE EXAMPLES OF BEHAVIORAL MODE

GENERAL

The discussion in this section is an effort to compare the Phase 1 and Phase 2 behavior of cylinders which fracture completely in shear with cylinders which fracture in a combined tensile-shear mode. Data were available for cylinders of SAE 1015 steel which were fired when the loaded cylinders were at three different temperatures: normal (about 80°F), -60°F, and -110°F (References 5 and 6). All of these cylinders used the standard test cylinder design previously given. The C/M ratios for the three cylinders were 0.85, 0.86, and 0.88, respectively. Chilling methods, chilling times, and temperature monitoring techniques for the loaded cylinders used for these studies are described in Reference 3.

Fracture behavior was affected by temperature in the following manner (Reference 3). The cylinder fired at normal temperature fractured in the typical all-shear fracture mode. The two low temperature firings both fractured in the combined tensile-shear mode. For the -60°F test the outer tensile portion had an average depth inward from the outer surface of 25 percent of the fragment thickness, with the inner 75 percent of the wall fracturing in shear. For the -110°F test the corresponding average values were 35 percent in tension and 65 percent in shear. Sketches of typical fracture formation in cylinder cross sections for these three behavioral modes are shown in Figure 3. A comparison of cylinder behavior for the normal temperature and -110°F temperature test as taken from Cordin camera records is given in the following sections.

SHEAR FRACTURE BEHAVIOR

The typical behavior for a plain wall cylinder of SAE 1015 steel fired at normal temperature (about 80°F) was as follows. As the detonation front passed a given section of cylinder, the wall began to move outward (start of Phase 1). When that section had increased about 18 to 20 percent on the outside diameter, shear fractures first appeared on the outside surface (start of Phase 2) and then propagated inward through the wall of the cylinder. Starting as axially-oriented hairline fractures, with successive frames these fractures increased in number, and each fracture grew in length and width until it became obscured by the products emerging from the mouth of the fracture. Detonation products first appeared in the fracture opening when the case section had increased about 60 percent total on the diameter (start of Phase 3).

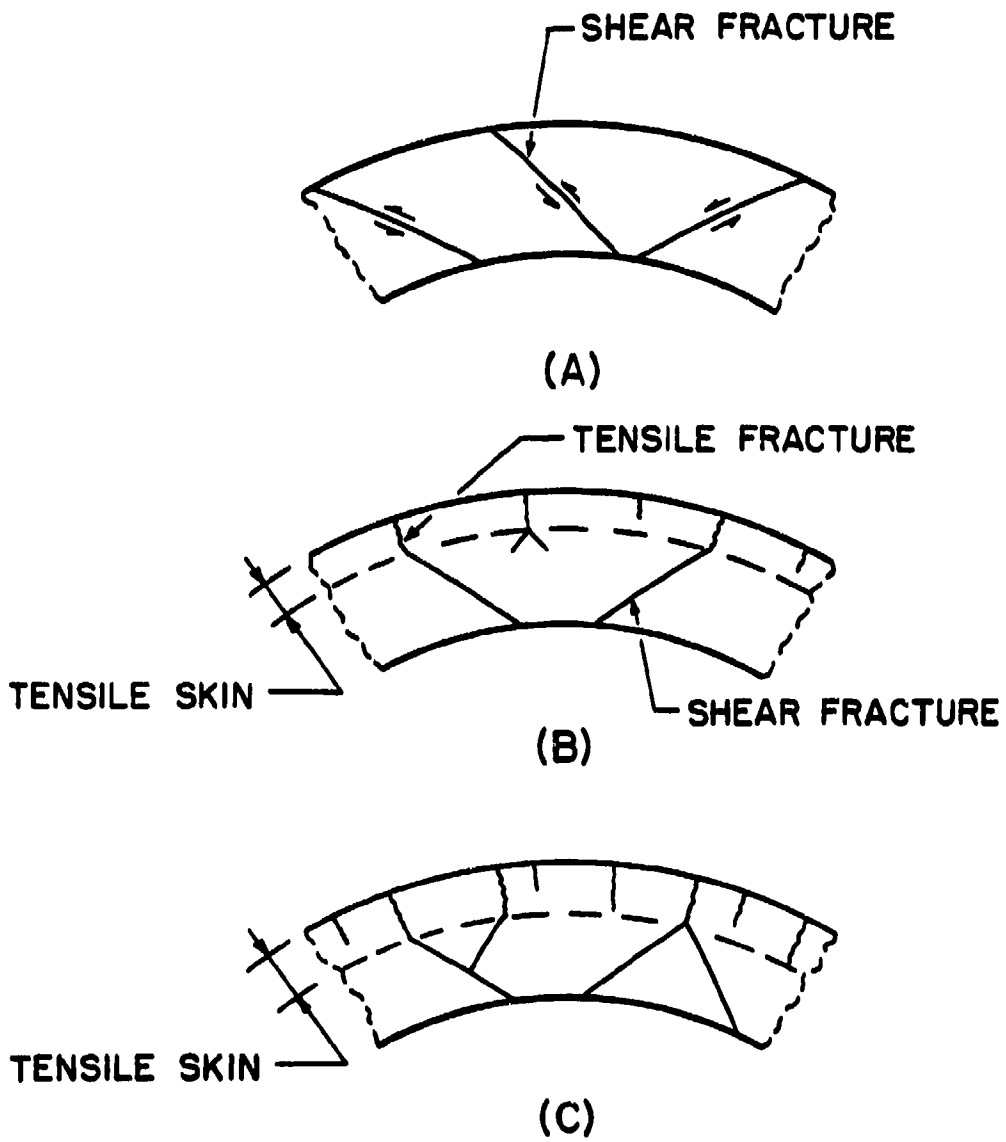

FIGURE 3. Fracture Patterns in Cylinder Walls for (A) +80°F, (B) -60°F, and (C) -110°F.

Time durations for Phases 1 and 2 were as follows. From the first sign of case expansion to the first sign of fracture took about 9 microseconds. This was the time duration of Phase 1. Detonation products first appeared 15 to 18 microseconds after the appearance of the first fractures. This was the time duration of Phase 2. Thus, Phase 3 started at 24 to 27 microseconds after the first sign of case expansion.

Table 1 lists fracture dimensions for the early growth of three prominent shear fractures visible on the outer surface of the cylinder during the Phase 2 period. These fractures were located at distances of about 2 1/4, 5, and 8 inches from the detonator end. Starting as an axially-oriented hairline crack, each fracture grew with a narrow elliptical shape which had fairly sharp ends. The table shows the initial length and width for each fracture as it first appeared, and the fracture dimensions at the time that detonation products began emerging from the fracture, thus covering fracture growth during Phase 2, a time period which lasted 15 to 18 microseconds. This type of fracture growth behavior can be seen by following specific fractures in the pictures of Figure 1. Additional growth of the fractures, and the subsequent joining of the fractures to form discrete fragments, events which occurred in Phase 3, were obscured by the detonation products. Figure 4 shows the cross section of a fragment recovered from a normal temperature test of the type discussed here. Both sides of the fragment are the result of full shear fractures, and the cross section of the fragment indicates fully ductile behavior.

TABLE 1. Growth of Surface Fractures During Phase 2.

Distance from detonator end, in.	Start of Phase 2		End of Phase 2	
	Length, in.	Width, in.	Length, in.	Width, in.
2 1/4	5/8	Hairline	1	3/16
5	3/8	Hairline	1 1/8	3/16
8	9/16	Hairline	1 3/16	5/32

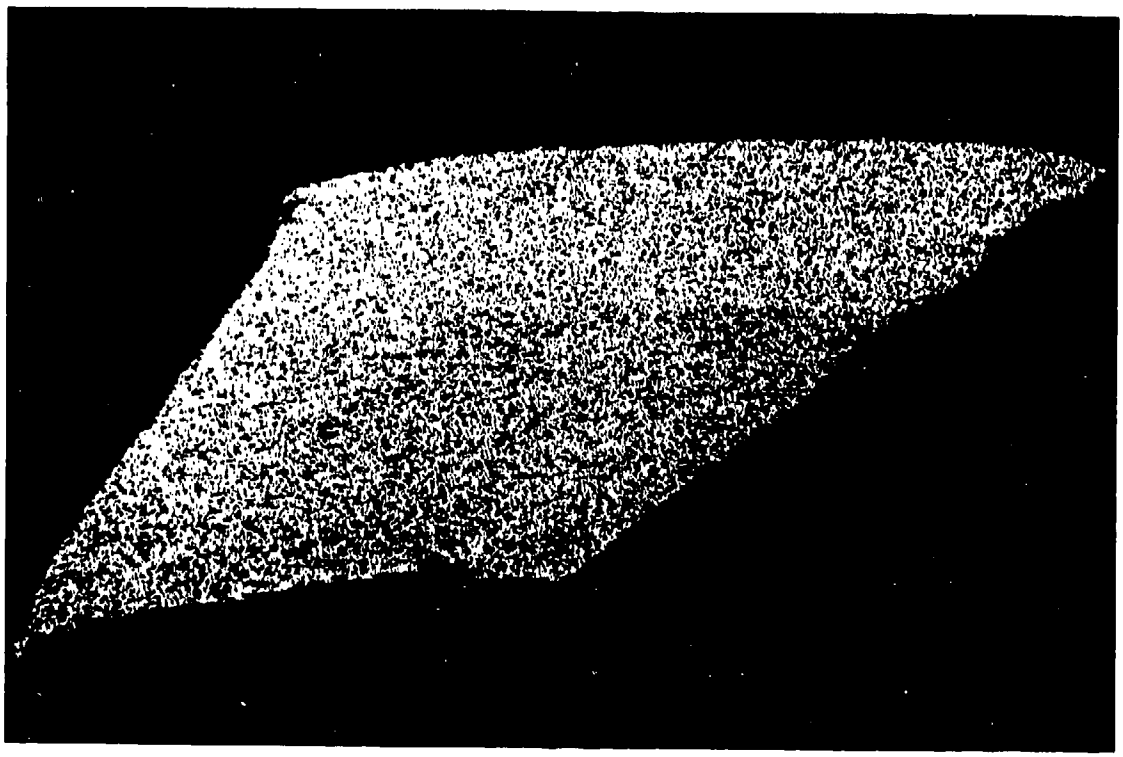

FIGURE 4. Cross Section of Fragment From Normal Temperature(+80°F) Cylinder Showing All-Shear Fracture Behavior. Inner surface at bottom of picture.

COMBINED TENSILE-SHEAR FRACTURE BEHAVIOR

For a plain wall cylinder of SAE 1015 steel tested at about -110°F, the fracture behavior was influenced by the presence of an outer tensile layer which extended inward from the outside surface for an average depth equal to about 35 percent of the fragment thickness. The fractures formed in this outer 35 percent zone were all tensile fractures. The fractures formed in the inner 65 percent ductile portion of the wall were all shear fractures. Those fractures which extended completely through the wall were a combination of tensile and shear types.

The axially-oriented hairline fractures which first appeared on the outer surface of the cylinder (start of Phase 2) at about 20 percent increase on the diameter were all tensile breaks. Detonation products began to emerge from the fracture openings at about 65 percent total increase on the diameter (start of Phase 3). Corresponding times were again approximately 9 microseconds from

the start of metal displacement to first fracture (Phase 1), and about 18 microseconds additional to the first sign of detonation products visible in the mouth of the fracture (Phase 2).

The surface fractures which initially formed in any given section of the low temperature cylinder were far greater in number, and individually less distinct than for the normal temperature cylinder which showed all shear fractures. While the shear fractures which formed at normal temperature grew in length as individual, rather easy-to-follow fractures during Phase 2, the low temperature tensile fractures grew as an overall interacting field through the extensive and hard-to-follow linking together of many short sections. Meaningful measurements of individual fracture growth during Phase 2 were not obtainable. The size of the major fragments, however, was determined by the shear fractures which formed in the inner portion of the cylinder wall and linked up with corresponding tensile breaks in the outer layer. This can be seen in Figure 5, which shows the cross section of a fragment from a low temperature (-110°F) test. The ductile and brittle zones, and the associated shear and tensile fractures, are clearly evident. The left and right sides of the fragment are the result of combined tensile-shear fractures.

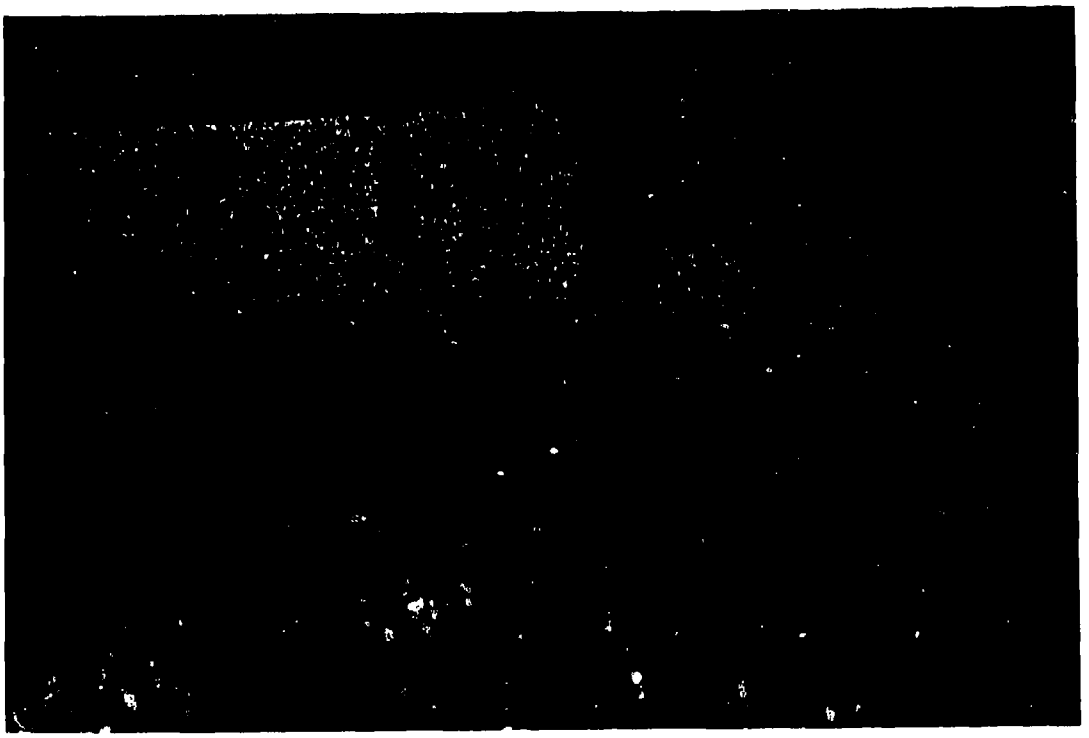

FIGURE 5. Cross Section of Fragment From Low Temperature (-110°F) Cylinder Showing Combined Tensile-Shear Fracture Behavior. Inner surface at bottom of picture.

Table 2 compares the time durations and diametral increases during Phases 1 and 2 for the all-shear fracture behavior (normal temperature) and the combined tensile-shear fracture behavior (-110°F). The results are strikingly similar, based on equal framing rates of 333,000 frames per second for both studies.

TABLE 2. Cylinder Data for Phases 1 and 2.

Loaded cylinder temp., °F	Fracture type	Phase 1		Phase 2		Total	
		Duration, μsec	Diametral expansion, %	Duration, μsec	Diametral expansion, %	Duration, μsec	Diametral expansion, %
80	All-shear	9	20	15-18	40	24-27	60
-110	Combined tensile-shear	9	20	18	45	27	65

ADDITIONAL THOUGHTS ON CASE EXPANSION

Probably the first detailed discussion of steel cylinder expansion behavior was given by Taylor in 1944 (References 8 and 9). This was based on some high-speed photographic work attributed to D. P. MacDougall and G. H. Messerly who used flash photography with an exposure time of the order of 1 microsecond (Reference 8) to view the expansion of steel cylinders loaded with 50/50 cast pentolite. Taylor's data were based on the study of three different wall thicknesses, 1/16, 1/8, and 1/4 inch, with a fixed ID of 1 1/2 inches. Taylor's values, based on the use of reflection photography (Reference 9), gave the first appearance of the detonation products (end of Phase 2) when R_2/R_0 = 1.76 to 2.0, or about 76 to 100 percent expansion of the cylinder.

Stronge (Reference 10) generalizes that for ductile steel cylinders of about the size given earlier in this report, fracture initiation starts at the outer surface when R_1/R_0 = 1.3, or about 30 percent cylinder expansion, and that the detonation products appear at a burst radius of R_2/R_0 = 1.7, or about 70 percent expansion.

In the author's studies (Reference 5), previously described, using a Cordin camera to study the behavior of plain, ductile steel cylinders, Phase 1 ends when R_1/R_0 = 1.2, or 20 percent expansion, and Phase 2 ends when R_2/R_0 = 1.60 to 1.65, or 60 to 65 percent expansion. In the above ratios the symbols R_2, R_1, and R_0 represent the outer radius of the cylinder wall at the end of

Phase 2, the end of Phase 1, and in the original undeformed condition, respectively.

Table 3 compares the data from these different sources for the percent expansion of the cylinder at the end of Phase 2. It shows that for experimental studies spanning a period of 45 years, with different photographic techniques, different cylinder sizes, and different explosives, the expansion values are surprisingly similar.

TABLE 3. Cylinder Expansion at the End of Phase 2.

Source	Expansion, %	Reference
Taylor (low range)	76	9
Stronge	70	10
Pearson (high range)	65	5

In comparing data from different sources for cylinder expansion at the end of Phase 2, an additional factor needs to be considered. In the analysis of photographic records for establishing the end of Phase 2, the investigator can determine the end condition by using either of two approaches. These are (1) when the products "bubble" first appears fully in the mouth of the fracture but is not yet visible in the cylinder profile, or (2) when the products have just cleared the surface of the cylinder and are first visible in profile. These two approaches are currently representative of studies using high-speed framing camera or high-speed streak camera techniques, respectively. In earlier studies which used single frame flash photography these two approaches were represented by frontal lighting (reflection photography) or back lighting (shadow photography), respectively.

The author's analysis used the first approach. In the author's studies the difference in the first appearance of the products, i.e., frontal viewing versus profile viewing, was represented by one interframe (i.e., 3 microseconds or less). This one frame difference had the effect of increasing the expansion value in Table 3 from 65 percent to about 73 percent and represents the expansion range, depending on which analysis approach was used at that framing rate.

VELOCITY MODE

BACKGROUND

In 1943 R. W. Gurney of the Ballistics Research Laboratory (BRL) published a report (Reference 11) for the predicted values of fragment velocities from explosively filled cylinders. The velocity derivation was based on an energy balance in which a cylinder of infinite length is filled with an explosive of uniform density which is axially detonated simultaneously along its length. The energy released by the detonating explosive is equated to the kinetic energy of the case and the detonation products, and from this energy balance an expression is obtained for the radial velocity of the case.

The Gurney equation takes the form

$$V_G = \sqrt{2E}\left[\frac{C/M}{1 + 0.5\,C/M}\right]^{1/2}$$

where V_G, E, C, and M are defined as the initial casing velocity, the energy content of the explosive, the explosive mass, and the casing mass, respectively.

The term $\sqrt{2E}$ is normally referred to as the "Gurney Constant." The value of this constant varies with the explosive type and also with the explosive density. Values for this constant are empirically determined and can be found in the literature for a wide range of explosives (References 12 through 15). Reference 15 includes a particularly extensive list. Excellent reviews of the Gurney type equations, their derivations and applications, are given in References 12, 13, 14, and 16.

Since this radial velocity is obtained for the expanding cylinder prior to the formation of any fractures and before any release fronts can occur, it is typically referred to as the initial case velocity. However, Gurney titled his report "The Initial Velocities of Fragments from Bombs, Shells and Grenades," thus implying that the initial case velocity and the initial fragment velocity were the same. This interpretation has continued for several decades, with numerous authors using the two terms interchangeably, frequently within the same paragraph. However, the Gurney derivation does not take into account any acceleration phase of the cylinder wall, nor any velocity behavioral aspects which may be related to the fragmentation process. Thus, one approach might conclude that the derivation of the Gurney expression might conceivably place the velocity value at the end of Phase 1 in the behavioral mode, or even at the end

of Phase 2 with a slightly different interpretation, i.e., relation to fracture initiation versus relation to initial products release through fracture.

Taylor in one of his early reports written for the British Ministry of Supply in 1941 (Reference 17) suggested that the initial fragment velocity might be the same as the velocity of the case at the time of "burst." From the study of other papers by Taylor (References 8, 9, and 18) his meaning for terms such as "burst," "bursting," "burst point," and "burst ratio" all relate to the instant at which the detonation products first appear as they emanate from the fractures in the case. This would place Taylor's suggestion regarding the initial fragment velocity to the case velocity at the end of Phase 2.

Additionally, several other velocity interpretations have been offered. Kinney and Graham (Reference 19) relate the Gurney velocity to the velocity of the casing fragments at the time of "break-up," which could be interpreted as either the burst point (end of Phase 2) or as some point in the fragmentation process, probably in the early part of Phase 3. Kennedy (Reference 13) refers to the Gurney model as one developed to predict the terminal velocity of fragments, which would place it in Phase 4. Stronge, et al (Reference 10) considers the Gurney velocity as the upper bound on the speed of fragments that can be achieved from the case. This interpretation by Stronge is more in agreement with the approach suggested later in this report. It is also an approach which may best place the Gurney velocity value within the detonation products cloud, or Phase 3. Thus, depending on the interpretation of various investigators, the use of the Gurney velocity has been related to case velocities at the end of either Phase 1 or Phase 2; or to fragment velocities within Phase 3 or Phase 4.

The Gurney equation has been applied mainly to fragment velocity studies of relatively long standoff distances, usually for distances substantially beyond the limits of the detonation products cloud. As Crabtree and Waggener point out (Reference 14), the formulas developed by Gurney nearly 50 years ago have been surprisingly effective and useful for studies involving many different explosives and over a wide range of C/M values. Even today, if experimental velocity values are not available, the first thing the ordnance engineer reaches for is the Gurney equation. Also, the Gurney approach is particularly valuable to warhead designers by providing a quick, simple, and effective means for predicting how design changes which affect the C/M value, or a change in the type or amount of explosive load, can affect warhead performance.

It is of historical interest to note that both Gurney and Taylor worked, independently, on the fragment velocity problem in the early days of World War II (WW II). Both used an energy balance relation as the basis for their derivations. While Taylor's work on the fragmentation behavior of bombs and warheads (Reference 9) has been used as the basis for studies regarding the stress state

in the expanding case (for example, see Reference 20), it is Gurney's work that has been most often referred to in fragment velocity studies.

EXPERIMENTAL STUDIES

Multi-Flash Radiography

Waggener (Reference 21) used multi-flash radiography to obtain fragment velocities within the detonation products cloud. For example, in his studies a mild steel cylinder with a small-diamond, inner surface grid was loaded with Comp C-3 explosive and single-point, end initiated. The cylinder was 76-mm OD, had a wall thickness of 2.54 mm, and an L/D value of 1.25. The C/M value for the loaded cylinder was 1.42.

Velocity measurements were based on fragment positions at two different times, between 130 and 450 microseconds after initiation, which should place the fragment measurements well within the detonation products cloud. The maximum fragment velocity obtained from the velocity profile occurred at a location at about L/2, and was approximately 95 percent of the calculated Gurney velocity for that cylinder.

Cordin Camera Measurements

The same Cordin camera records which were used to obtain an understanding of the early stages of the case expansion and fragmentation process can also be used to estimate case velocities in Phases 1 and 2 of the behavioral process. The problem that arises from this approach is the possible experimental error which can exist when comparing a sequence of pictures, each having an effective exposure time of about 3/4 microsecond when the interframe time is only 3 microseconds. The possible motion which can occur during the exposure time is about 25 percent of the motion which occurs during the interframe time. However, by projecting the 35-mm frames onto the glass screen of a large back-surface analyzer and by using a standard procedure for obtaining diametral measurements from the images, approximate values of case velocity can be obtained.

More precise values of case velocity could be obtained using high-speed streak camera photography. Perhaps the ideal approach would be to coordinate both (a) high-speed framing camera photography and (b) high-speed streak camera photography of the same event so as to relate both the physical behavior from (a) with the velocity behavior from (b). This has not been done. The following example is based on velocity measurements taken from the projected images of Cordin camera frames for Phases 1 and 2 and the use of data from other sources for Phases 3 and 4.

Due to end losses in a cylinder of finite length, the Gurney equation relates best to the central portion of cylinders with L/D of two or greater, where D is taken as the inside diameter of the cylinder (Reference 14). In the velocity examples for Phases 1 and 2 given in this report, case velocity values are representative of the center portion of the cylinder in the region near L/2.

REPRESENTATIVE EXAMPLES OF THE VELOCITY MODE

Shear Fracture Behavior

Velocity-distance data for two cylinders of SAE 1015 steel were obtained from the types of tests previously described. One of the cylinders provided Zone 4 velocity data which were obtained from an arena test using split-frame Fastax cameras to determine fragment velocities (Reference 1). Data for Zones 1 and 2 were obtained from the second cylinder using a Cordin camera and represents behavior at a location 5 inches from the detonator end, or at L/2. Velocity data for Zone 3 were based on the Gurney value for these cylinders. The term V_R is used in the general sense to indicate a representative velocity for an unspecified zone. When a representative velocity relates to a specific zone it is given as V_1, V_2, V_3, or V_4.

Both cylinders were 5-in. OD x 4 1/2-in. ID x 10-in. long, loaded with Comp C-3 explosive, and single-point end initiated. Both cylinders had plain walls and correspond to the shear fracture behavior example previously discussed. Each of the loaded cylinders had a C/M value of about 0.85 and a calculated Gurney velocity of about 6,800 ft/sec.

The velocities taken from the Cordin camera records for Zones 1 and 2 are representative values for these zones or phases. These velocity values were obtained by using a straight line fit through the diametral measurements given as a function of time for the two phases. This procedure always provided a natural break, or point of intersection, in the velocity lines at a point in the plot which correlated with the onset of fracture at the outer surface of the cylinder (i.e., end of Phase 1).

To determine the Gurney velocity the Gurney constant, $\sqrt{2E}$, was taken as 8,800 ft/sec for Comp C-3 explosive (References 13, 15, and 21). If the 95 percent value obtained by Waggener (Peference 21) also applies to plain wall cylinders, then V_3 for the two cylinders considered here would be about 6,450 ft/sec. It may be more realistic to say that V_3 is somewhere between 6,450 and 6,800 ft/sec, using Stronge's approach (Reference 10) that the Gurney velocity represents the upper bound for the fragment velocity. The representative value for Zone 4 was taken as the fragment velocity averaged over 20 feet from

warhead to target (Reference 1). The Zone 4 velocity values are based on the arrival of the first "family" of fragments at the targets, rather than the few precurser fragments which frequently occur and which may have a velocity some 3 to 5 percent higher.

One approach for establishing reference velocities for each zone is to assume that the Gurney velocity either exists or is very closely approached in Zone 3, and relate the velocities in Zones 1, 2, and 4 as some fraction of the Gurney velocity.

Thus, for Zone 1, $V_1 = \beta_1 V_G$;
Zone 2, $V_2 = \beta_2 V_G$;
Zone 3, $V_3 = \beta_3 V_G$, or $V_3 = V_G$; and
Zone 4, $V_4 = \beta_4 V_G$;

where the velocity constants β_1, β_2, β_3, and β_4 are experimentally determined.

Table 4 gives the representative zone velocity values obtained by the above approach and also lists each value as a percent of the Gurney velocity.

TABLE 4. Representative Velocities for Zones 1 to 4. (Shear Fracture Behavior)

Zone no.	Representative velocity, V_R, ft/sec	Percent of Gurney velocity, V_R/V_G
1	4,100	60
2	5,400	80
3	6,450-6,800	95-100
4	6,200	91

Combined Tensile-Shear Fracture Behavior

Behavior for the cylinders described here corresponds to the combined tensile-shear fracture example previously discussed for plain wall cylinders. The velocity data were obtained in the same way as described in the previous section.

Two cylinders of SAE 1015 steel loaded with Comp C-3 explosive were pre-chilled to about -110°F and detonated. One of these cylinders provided Zone 4 velocity data which were obtained from Fastax camera records taken from an arena test in which the distance from warhead to target was 20 feet (Reference 3). Behavior of the second cylinder was studied by means of high speed photography as previously described. Velocity values for Zones 1 and 2 were again determined using straight line fits of diametral measurements of the expanding case. The location studied was 5.1 inches from the detonator end, essentially at L/2. Velocity data for Zone 3 were again based on the Gurney values for these cylinders.

Both cylinders were 5-in. OD x 4 1/2-in. ID x 10-in. long, as in all of the previous tests. When loaded with Comp C-3 explosive the cylinders had C/M values of 0.88 for the arena test and 0.86 for the Cordin camera study. Corresponding Gurney velocity values were about 6,880 ft/sec and 6,820 ft/sec, respectively, with an average value of 6,850 ft/sec, which was used as the upper limit for Zone 3.

Table 5 gives the representative zone velocity values which were all obtained in the same manner as for Table 4.

TABLE 5. Representative Velocities for Zones 1 to 4. (Combined Tensile-Shear Fracture Behavior)

Zone no.	Representative velocity, V_R, ft/sec	Percent of Gurney velocity, V_R/V_G
1	4,200	61
2	5,500	80
3	6,500-6,850	95-100
4	6,150	90

The velocity ratio values, V_R/V_G, given in Tables 4 and 5 are almost identical for corresponding zones. For the four tests upon which the velocity values of these two tables are based, there are both marked differences and marked similarities. Large differences were present in the temperatures of the loaded test cylinders and in the related brittleness/ductility ratios of fracture. However, the C/M values were extremely close, with an overall spread of only 0.85 to 0.88, and the same explosive was used in all tests.

From the data presented in Tables 4 and 5 the velocity results of these four tests all fit the following general patterns.

$V_1 = 0.6\ V_G$
$V_2 = 0.8\ V_G$
$V_3 = 0.95\ V_G$ to $1.0\ V_G$
$V_4 = 0.9\ V_G$

It is not known how well these ratio patterns would apply to warheads of different dimensional sizes or to those loaded with different explosives. However, since both of the most important velocity parameters, i.e., the C/M ratio and the Gurney constant, are accounted for in the V_G value, these ratio patterns should provide simple velocity estimates, or at least serve as a point from which to start a velocity determination.

PUTTING IT ALL TOGETHER

GENERAL MODEL

Figure 6 shows a way of presenting the fragmentation model by combining the fragmentation mode and the velocity mode into a general spectrum of behavior. Points A, B, C, D, and E represent the start and end points for both the behavioral phases and the velocity zones. The horizontal axis represents both time and distance. The velocity values for Zones 1 through 4 are representative values for each zone, which are obtained as previously described. End conditions for each of the zones or phases are experimentally established, as discussed in the Behavioral Mode section of this report..

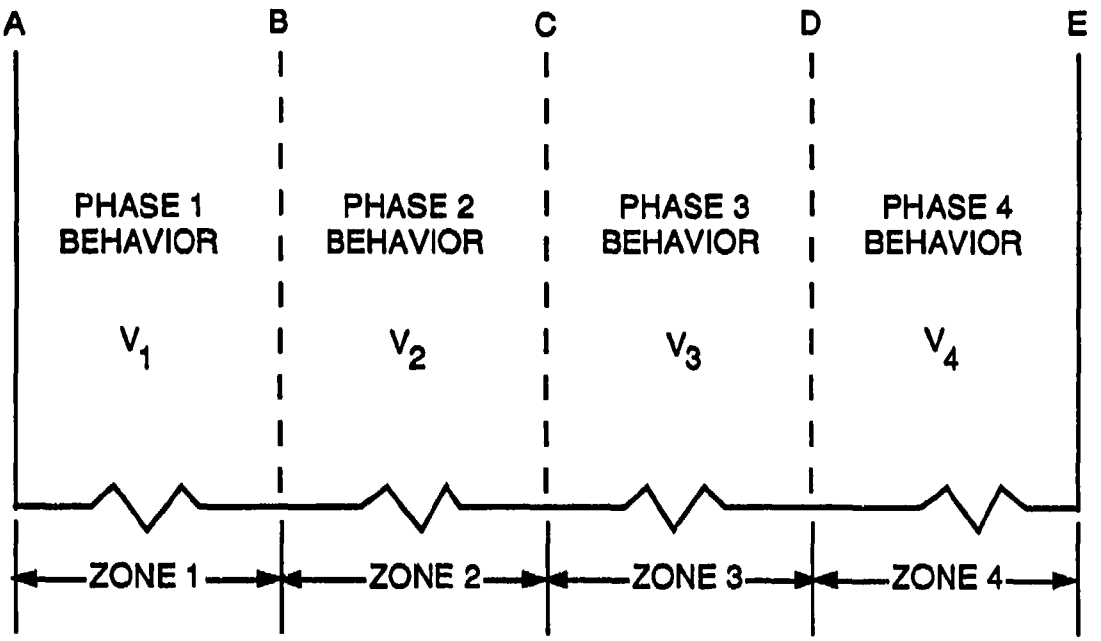

A - First radial motion of case section.
B - First sign of fracture on outer surface.
C - First sign of detonation products from fractures.
D - Fragments leave the detonation products cloud.
E - Target.

Phase 1 - Elastic-plastic expansion (no fractures).
Phase 2 - Growth of fracture system prior to appearance of products. Plastic expansion with opening fractures (no products).
Phase 3 - Continued case expansion in early phase, followed by major fragmentation process occurring in the detonation products cloud.
Phase 4 - Terminal flight of fragments.

FIGURE 6. Fragmentation Model Spectrum of Behavior.

SPECIFIC EXAMPLES OF THE FRAGMENTATION MODEL

Plain Wall Cylinder With All-Shear Fracture

By combining quantitative data previously presented for both the behavioral and velocity modes, full representation can be obtained for specific test cylinders previously discussed. For example, Figure 7 gives the fragmentation model for a plain wall cylinder of SAE 1015 steel which fractured completely in shear when tested at normal temperature. The early time and distance values for points A, B, and C were obtained from Cordin camera records (Reference 5). Values are based on the 3-microsecond interframe times. No attempt was made to interpolate between frames. Data for point E were taken from results of arena tests (Reference 1).

Time and distance data for point D could not be determined from the experimental results available. However, theoretical guides given by Kinney (Reference 22) can be used for estimating the limiting distance for the forward motion of the detonation products. Time and distance values given for point D in Figure 6 are based on this approach. Since it is expected that the fragments leave the products cloud prior to its achieving maximum size, these numbers represent limiting conditions.

The distance values for points A, B, C, and D are all given in terms of the original outer radius of the cylinder, R_0, since these distances are a function of cylinder size, in this case 2.5 inches. The distance for point E is given in feet since the distance from warhead to target is a fixed distance, in this case representative of the arena size. Time values for points B and C are given in microseconds, and for points D and E in milliseconds.

Velocity values for each zone were obtained as previously described. Values for V_1 and V_2 are straight line approximations taken from sequential diametral case measurements taken from Cordin camera records. The value for V_3 is based on the Gurney velocity for the cylinder, and V_4 is the averaged fragment velocity (V_{20}) taken from Fastax camera records of arena tests.

The physical nature of the warhead case or resulting fragments can be estimated for each of the four zones from the earlier discussion regarding the behavioral mode of the case. Each phase of behavior relates to the similarly numbered velocity zone, i.e., Phase 1 relates to Zone 1.

The terminal nature of the fragments is presented in Figures 8 and 9. Figure 8 shows a representative fragment grouping for this example. The fragments were recovered from Celotex modules in a 20-foot radius arena and represent the end condition of the original cylinder at Point E in Figure 7. Figure 9 shows the corresponding fragment mass-distribution plot, or fragmentation signature, for this example.

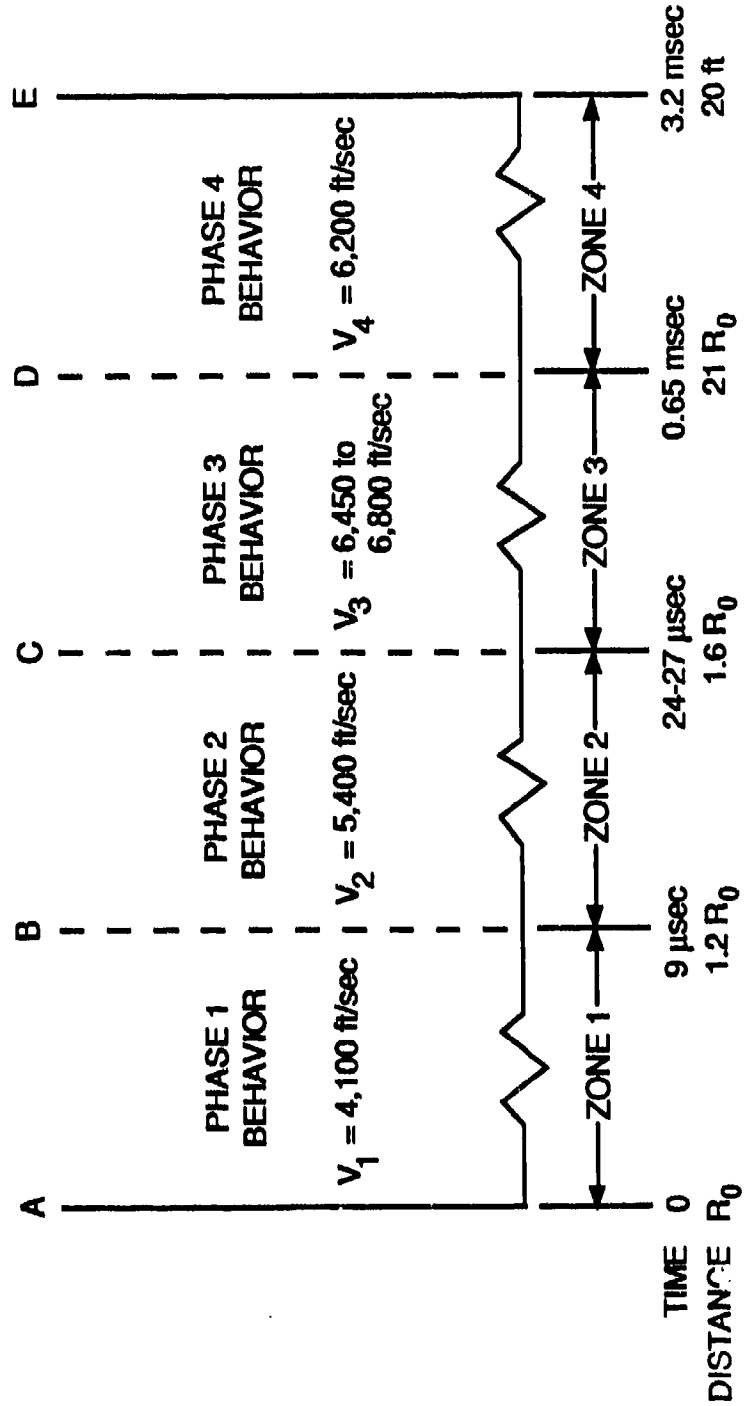

FIGURE 7. Fragmentation Model for All-Shear Fracture Behavior (+80°F).

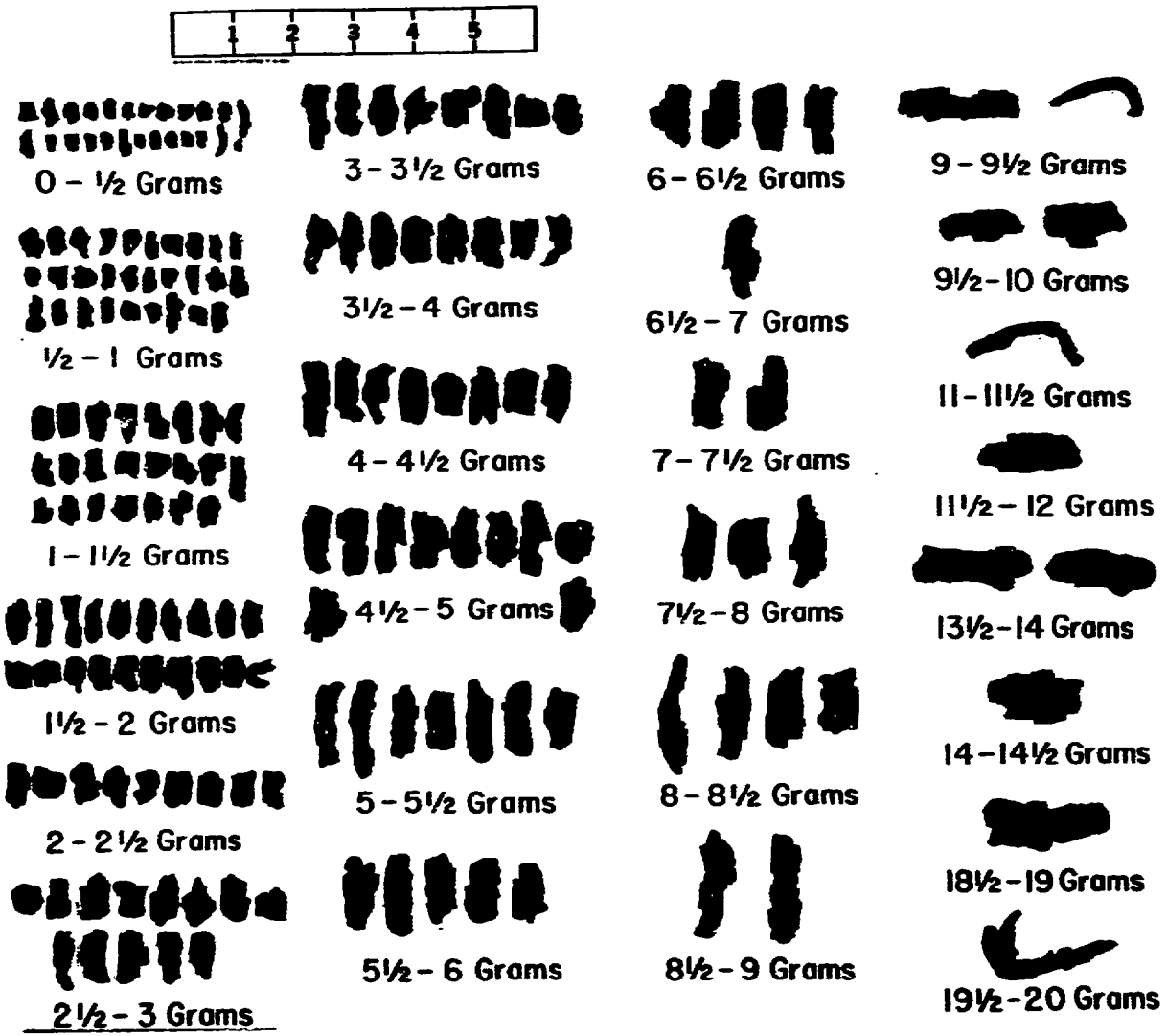

FIGURE 8. Fragments From All-Shear Fracture Example.

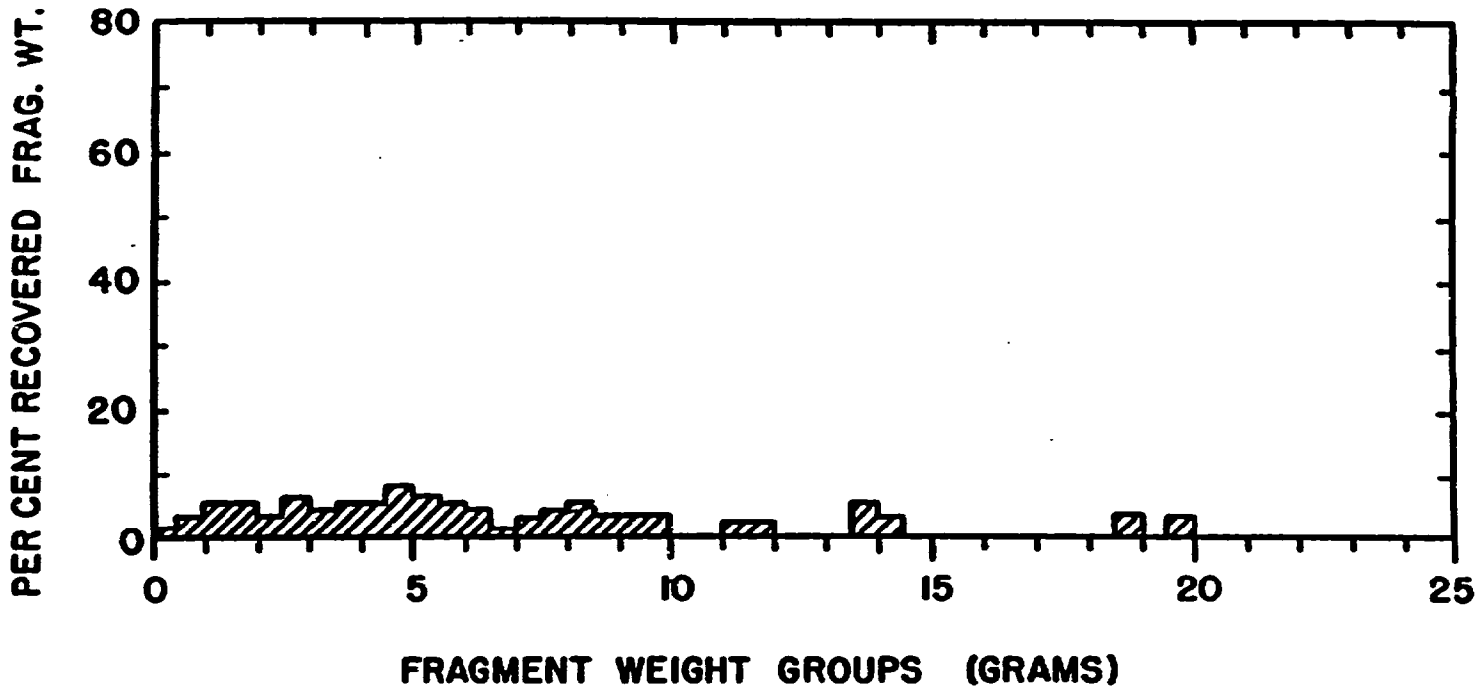

FIGURE 9. Fragmentation Signature for All-Shear Fracture Example.

Plain Wall Cylinder With Combined Tensile-Shear Fracture

Figure 10 represents a similar fragmentation model for a plain wall cylinder of SAE 1015 steel where combined tensile-shear fracture behavior was achieved by pre-chilling the loaded cylinder to an overall stable temperature of about -110°F. All of the data were obtained in the manner described for the previous example. Data for point E were taken from the results of 20-foot arena tests (Reference 3).

Again, the physical nature of the warhead case or the resulting fragments for each of the four zones can be estimated from the behavioral mode of the cylinder. However, for this example the presence of an outer tensile portion of the cylinder wall needs to be considered. In general, the effect of the tensile skin is to increase the number of outer layer fractures which occur in Phase 2, a condition which continues into Phase 3 (References 3 and 5). This behavior needs to be superimposed on the descriptive behavior previously presented for the all-shear fracture example.

The overall effect from this type of behavior is to produce somewhat smaller and more numerous fragments. This can be seen from the terminal nature of the fragments presented in Figures 11 and 12. Figure 11 shows a representative grouping of fragments for this example. Recovered from Celotex modules in a 20-foot radius arena, they represent the end condition of the cylinder at Point E in Figure 10. Figure 12 shows the corresponding fragment mass-distribution plot for this example. A comparison of the fragment mass-distribution plot in Figure 12 to the plot in Figure 9 shows how this type of fragmentation behavior has moved the centroid of the plot to the left in Figure 12 resulting in a smaller average fragment size from that in Figure 9.

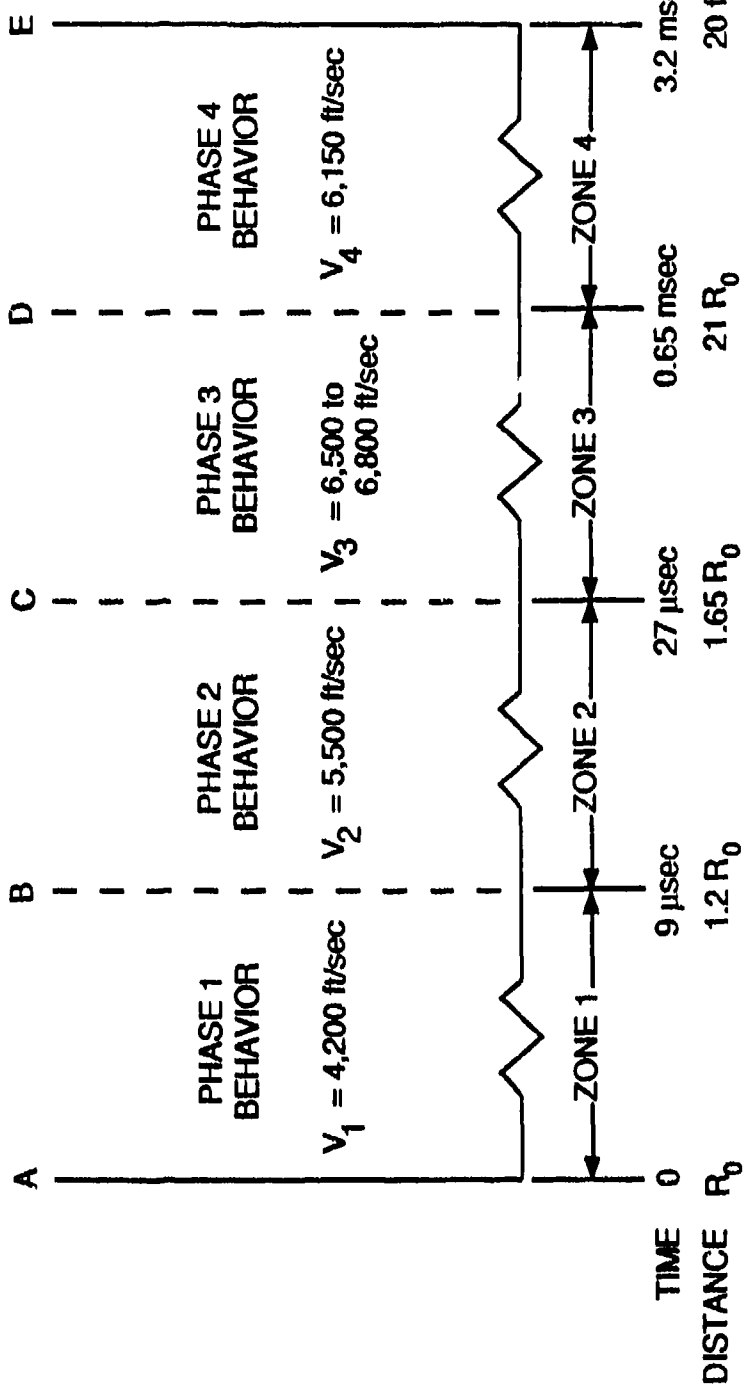

FIGURE 10. Fragmentation Model for Combined Tensile-Shear Fracture Behavior (-110°F).

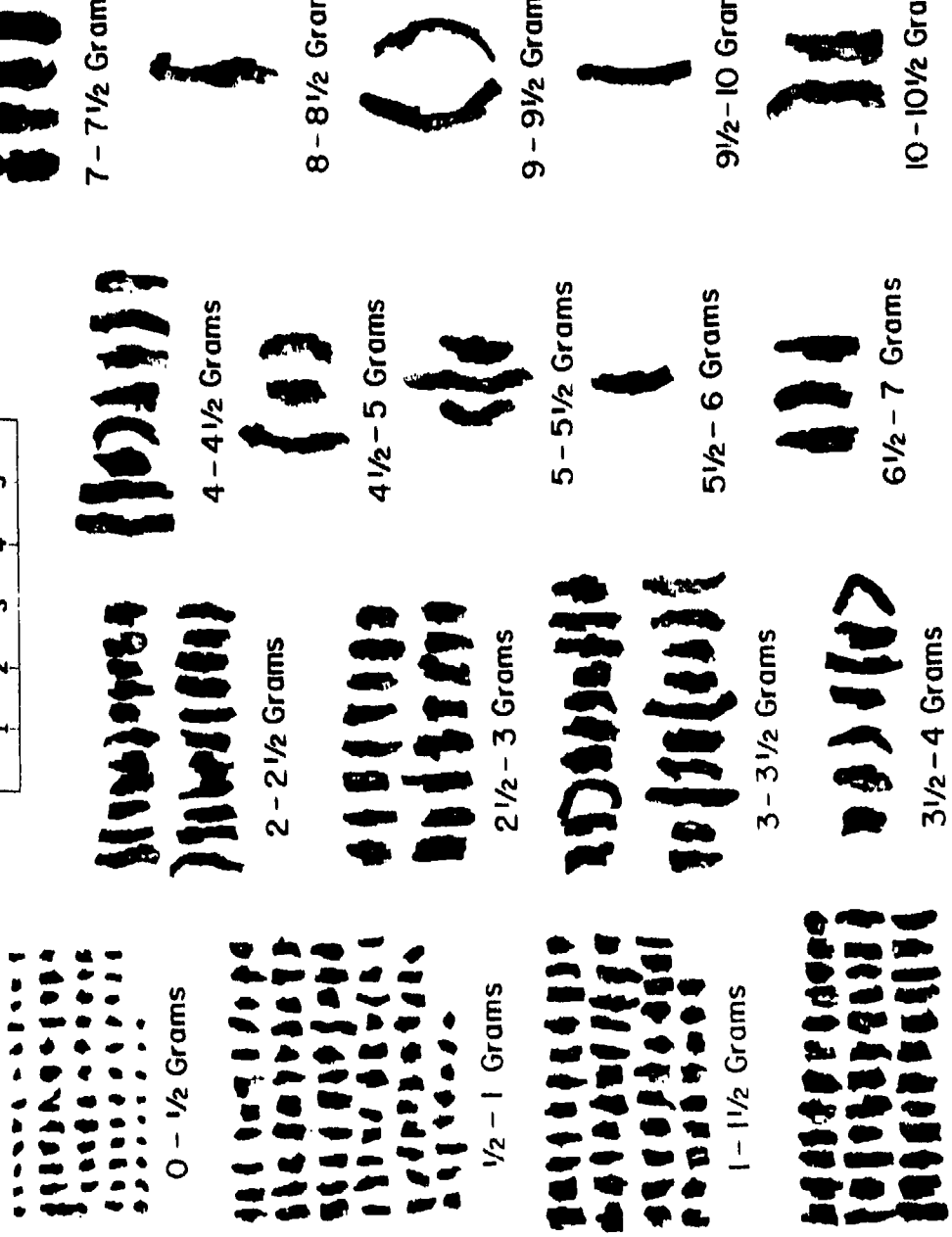

FIGURE 11. Fragments From Combined Tensile-Shear Fracture Example.

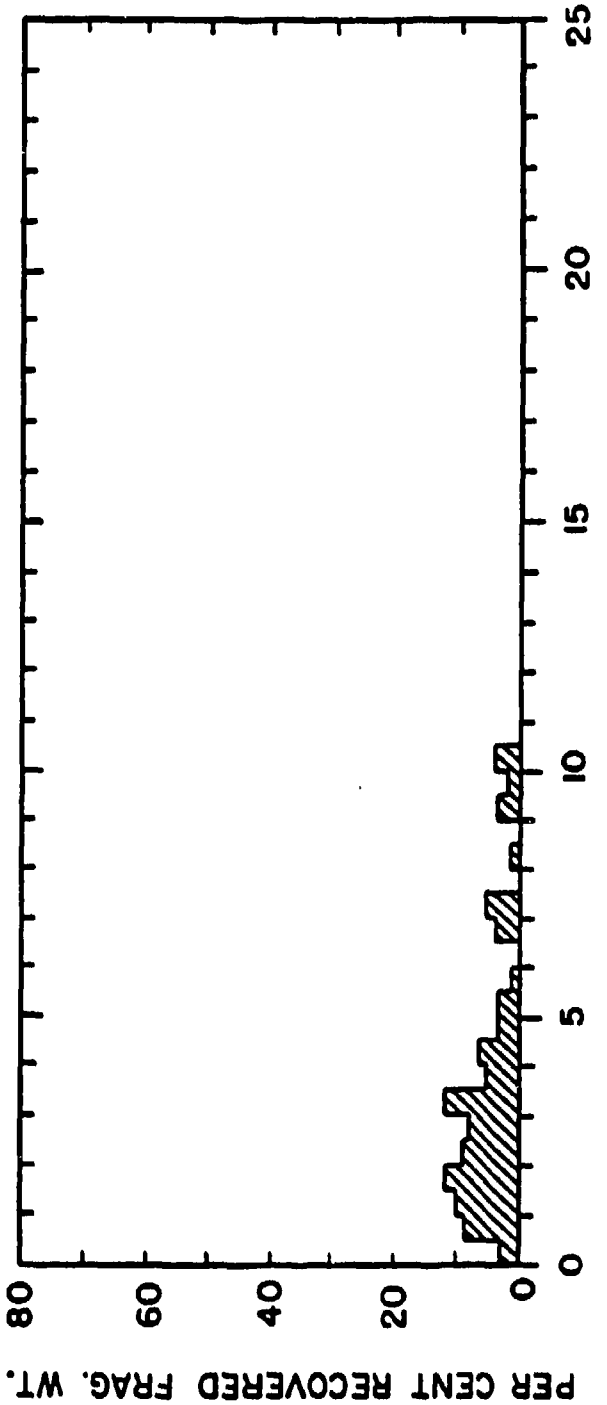

FIGURE 12. Fragmentation Signature for Combined Tensile-Shear Fracture Example.

OTHER CONSIDERATIONS

In order to better understand the conditions which govern the physical behavior of the warhead case after the start of detonation and the resulting velocity of the fragments, some additional behavioral aspects need to be considered. The information presented in the following sections can be interwoven, as seems necessary, into the fragmentation model previously discussed.

THE TAYLOR EXPANSION CONCEPT

In 1941, Taylor (Reference 17) devised a method for determining the "efficiency" of a bomb as a projector of fragments in terms of the relative amount of detonation energy which theoretically could be transferred to the case as kinetic energy. He considered the limiting condition for fragment velocity to have been established when complete rupture of the case had occurred (end of Phase 2). Thus, the further the case expanded without rupture, the greater was the "efficiency" of the bomb, the greater was the amount of energy transferred to the case, and the greater was the case velocity. Thus, the longer the case held together in an elastic-plastic expansion (Phases 1 and 2), the greater would be the velocity of the resultant fragments.

This concept laid down by Taylor nearly 50 years ago is demonstrated today by the use of "check seals" in some types of fragmentation warheads, particularly those types involving the use of preformed fragments and rod bundles. Without the containment effect provided by such a cylindrical check seal inserted between the explosive and the metal components constituting the case, detonation products would immediately pass through between the component members of the case, and the energy transferred from the detonation products to the preformed fragments would be substantially reduced.

A number of investigators have commented on this reduction in the fragment velocities of preformed fragments. For example, Waggener in his fragment velocity studies with solid cylinders and preformed fragments (Reference 21) came to the conclusion that "Warheads constructed of preformed fragment cases produced fragment velocities approximately 10 percent lower than similar warheads of solid cases." In Waggener's studies steel cubes were placed directly on the Comp B explosive charges without the presence of any check seal. In other studies by the author (not referenced here) where a relatively thin and low strength cylindrical check seal was used, the velocity reduction for preformed case components compared to fragments from solid cylinders approached 20 percent.

Other investigators relate the velocity loss for preformed fragments through the value of the Gurney constant used in their calculations. Henry notes (Reference 16) that if the fragments from a cylindrical case are preformed, the value for the Gurney constant $\sqrt{2E}$ is reduced by 10 to 15 percent to take into account gas leakage. For the same sort of situation involving the early release of the detonation products, Kennedy (Reference 13) indicates that the effective value of the Gurney constant may be decreased by as much as 20 percent. Such a reduction in the Gurney constant would give a corresponding reduction in the calculated Gurney velocity.

For warheads with a solid steel cylindrical case, the Bridgman effect (Reference 1) provides a natural check seal in the nature of a zone of ductile behavior in the inner portion of the cylinder wall. Even though the outer portion of the warhead case may be fracturing in tension, the inner ductile portion may still be expanding intact and thus containing the detonation products. As shown by prior examples in this report, the expansion ratios prior to "rupture" (end of Phase 2) for all-shear behavior at normal temperature and combined tensile-shear behavior at about -110°F were essentially the same, with a 60 to 65 percent increase in the diameter.

When comparable plain-wall cylinders, one at normal temperature and the other pre-chilled to about -110°F, were test fired in 20-foot radius arenas (Reference 3), fragment velocities averaged over 20 feet (V_{20}) for both types of behavior were essentially the same. The normal temperature cylinder which fractured in the all-shear mode had a C/M value of 0.85 and gave a V_{20} value of 6,200 ft/sec. The test cylinder which was pre-chilled to about -110°F fractured in the combined tensile-shear mode (35 percent tensile, 65 percent shear) as previously described. The low temperature test vehicle had a C/M value of 0.88 and gave a V_{20} value of 6,150 ft/sec. It might be concluded that the low temperature cylinder had a natural check seal which constituted the inner 65 percent of the case thickness and allowed the fragments to achieve essentially the same V_{20} value as the fragments from the normal temperature case.

From the data given in Table 1 of Reference 17, the behavior of these two examples, based on their rupture ratios, would have been given efficiency values of about 45 percent by Taylor's method of calculation. Taylor estimated that to get 50 percent of the available energy into the case it would be necessary for the case to "hold together" (end of Phase 2) until its diameter had increased by about 90 percent, that is $D_2/D_0 = 1.90$.

Thus, if this line of reasoning is applied, then to increase fragment velocities from a given warhead it becomes necessary to change the physical or engineering properties of the case in such a manner that the diametral ratio,

D_2/D_0, at the end of Phase 2 is substantially increased. The difficulties that arise in attempting this approach are briefly discussed later in this report.

It also indicates the problems which are encountered when trying to design a warhead where the velocities of preformed fragments compare favorably with the fragment velocities from a comparable warhead with a solid case. Fortunately, for this latter problem, the desirable features of controlled fragmentation offered by preformed fragments, and the higher fragment velocities offered by a solid case, can both be achieved through the use of inner-surface, shear-control grids (Reference 4).

THE BRIDGMAN EFFECT

Bridgman has demonstrated (Reference 23) that when high hydrostatic pressure is superimposed on a steel tensile specimen, the ductility and elongation characteristics of the specimen can be increased several hundred fold as compared to a similar specimen pulled to fracture at atmospheric pressure. To quote Bridgman on this subject: "Perhaps the most striking effect of hydrostatic pressure on such subs' nces as ordinary mild steel is the increase of ductility, that is the increase of plastic deformation which will be tolerated without fracture. . . . Under pressures in the range between 300,000 and 450,000 psi the degree of ductility which may be imparted is practically unlimited; in one instance an elongation of 300-fold at the neck was observed, without fracture."

Most of Bridgman's studies in this area relate to the WW II and post-WW II eras and involve the use of equipment whereby he could "pull" a tensile specimen while it was simultaneously subjected to hydrostatic pressures of up to 450,000 psi (Reference 24). The WW II studies appeared mainly as Watertown Arsenal and National Defense Research Committee (NDRC) reports dated from 1942 through 1944, while open literature papers on the subject appeared up to about 1950. All of this work, plus some of his very early studies starting about 1912, have been summarized and tied together in Reference 24. For example, in Table 5 of Reference 24, Bridgman documents the results of over 600 tensile tests conducted on steels under pressures ranging from atmospheric to about 425,000 psi. These studies included about 20 different steels, most of which were designated as being of "ordnance interest." Many of these steels were tested relative to different heat treatments with their resulting differences in properties. For example, SAE 1045, which was one of the steels of interest to Watertown Arsenal, was tested in nine different heat-treated conditions.

This geometry of a steel tensile specimen simultaneously subjected to a high hydrostatic pressure is also essentially realized in the wall of a warhead case during case expansion in parts of Phases 1 and 2, most notably near the inner surface of the case. Consider a circular cross section of the case as it

expands radially outward under the detonation pressure of an explosive. A circumferentially oriented element lying in the plane of the cross section near the inner surface of the case is simultaneously subjected to a tensile pull under the action of the circumferential stress, and to a large hydrostatic pressure effect resulting from the detonation pressure and the corresponding radial compressive stress in the wall of the case. This zone of ductility near the inner portion of the warhead case acts as a check seal, or pressure containment feature, particularly during the early part of Phase 2 during which fractures are propagating inward from the outer surface of the warhead case.

As a general rule the expansion behavior of a warhead case is treated as a problem in dynamic stress analysis, and numerous investigators, starting with Taylor (Reference 9), have studied it in this manner based on a variety of stress, strain, and energy criteria. Stronge (Reference 10) presents a condensed review of a number of these studies. In keeping with the purpose of this report, i.e., to treat the fragmentation model in a descriptive manner based on experimental results, the introduction of the Bridgman effect to explain the concept of a natural check seal in the warhead case seemed appropriate and, in the predictive sense, provides for the same general modes of behavior as the mathematical models. This approach based on Bridgman's studies was first presented by the author over 20 years ago (Reference 1) and has been used effectively by the author to quickly explain numerous problems related to warheads in their expansion and fragmentation behavior.

EFFECT OF CASE PARAMETERS ON FRAGMENT VELOCITIES

The fragment velocity equations as derived by Gurney, Taylor, Henry and others were based on an energy balance approach. The controlling parameters which appear in the relations are the C/M value of the warhead, and an energy constant for the explosive. The engineering and metallurgical properties of the case material do not enter into these velocity relations, except for the density of the case material which is accounted for in the C/M value.

Such behavior has been demonstrated experimentally in numerous Zone 4 velocity studies. For example, changing through wide ranges such properties of a steel case as hardness, strength, and the brittleness/ductility factor do not appear to noticeably affect the fragment velocity (Reference 1). Also, the type of steel used, ranging from the low-strength, plain low-carbon steels to the high-strength, heat-treatable types, which represent a wide spread of normally ductile to brittle behavior, appears to have little affect on fragment velocity (Reference 1).

Certain changes in the geometrical aspects of case design, attributable to the use of shear-control grids, can also be included in the above generalization regarding fragment velocity. Included in this are the following: (1) the use of shear-control grids on either the inner or the outer surface of the case (Reference 2), (2) different control sizes in the dimensions of the diamond pattern grids (References 1 and 2), and variations in the cross-sectional profile of the grid elements (References 1 and 2).

When the composite warhead (explosive and metal) has been chilled to extremely low temperatures (-60°F and -110°F) and detonated, fragment velocities remain essentially unchanged from normal temperature behavior (Reference 3). It is instructive to note in these low temperature studies that while the fragmentation behavior of the case is influenced by the presence of an outer tensile skin, considerable ductility remains in the bulk of the cylinder wall, so that the case does not shatter in the manner predicted from such behavioral tests as a temperature dependent Charpy impact test (References 25 and 26). This is an example of where the behavioral results taken from a conventional test can be partially or even completely overridden by the tremendous changes in the testing environment to which the metal is subjected by a detonating explosive. Numerous examples of such changes in behavior exist in the explosive ordnance field. Many of these examples were identified and explained about 35 years ago (Reference 27). However, with continuing advancements in the explosive ordnance field, what often seem to be new behavioral anomalies keep appearing. The investigator always needs to approach such apparent contradictions with an open mind.

All of the above parameters can produce marked changes in the nature of the fragments produced. The predominance in ductile shear fracture behavior can be changed to varying degrees of ductile-brittle combinations. The size and appearance of the fragments can change along with their respective fragmentation signatures (References 1 through 4), but the basic velocity of the fragments remains contained within a small experimental velocity spread (References 1 through 3), providing the C/M value and explosive energy constant are maintained. Excluded from the above velocity value generalization are possible velocity effects which can be obtained from such things as (1) initiation geometries specially designed to produce focussing effects, and (2) the degree of end confinement, which may affect the velocities of fragments at specific locations along the case.

As previously mentioned, the author has conducted numerous studies involving different engineering properties and different case design parameters, all based on the standard test vehicle described in the beginning of this report. As such, fragment velocities (V_{20}) can be easily compared based on changes in specific case parameters. The interested reader can find much of this earlier work, with extensive experimental results, presented in Reference 1 through 3.

AREAS OF APPLICATION

When a blast-frag warhead is detonated at some distance from a given target, the resulting terminal effects are largely dependent on the velocity and physical nature of the fragments, both of which have become essentially stabilized by the time of impact. This is the general encounter situation normally faced by the ordnance engineer and is representative of a Zone 4 encounter.

However, there are other situations where the velocity and the physical nature of the warhead case have not yet stabilized at the time of encounter. A general example would be when the warhead is detonated close enough to the target to place the encounter situation within Zones 1, 2, or 3. A more specific example would be the donor-receptor feature of stored munitions when one of the warheads is detonated inadvertently. In such a situation the warheads could be in close proximity, with separation distances ranging from a fraction of an inch to one or more diameters. This would also place the encounter situation within Zones 1, 2, or 3.

In the actual use of a blast-frag warhead, blast effect can be a major component of the total damage mechanism. Its effectiveness is a function of distance, being greatest in Zones 1 through 3, and decreasing with distance in Zone 4. Total damage to the target is the result of blast and fragment impact acting together in a synergistic manner. A major purpose of this report is to give the reader a better understanding of the warhead case behavior as a function of time and distance so that the case/fragment contribution can be factored better into the synergistic aspect of the total damage mechanism. Based on the fragmentation model described in this report, the actual times, distances, and metal velocities can be established for the warhead case in its different behavioral modes and can be shown by a plot similar to those in Figures 7 and 10. An appreciation for the combined blast-fragment effect can then be obtained by superimposing the fragmentation model plot onto blast wave plots involving pressure and impulse versus time and distance.

REFERENCES

1. Naval Weapons Center. *Parametric Studies for Fragmentation Warheads*, by John Pearson. China Lake, Calif., NWC, April 1968. (NWC TP 4507, publication UNCLASSIFIED.)

2. Naval Weapons Center. *Fragmentation Systems for Explosively Loaded Mild Steel Cylinders*, by John Pearson. China Lake, Calif., NWC, June 1969. (NWC TP 4764, publication UNCLASSIFIED.)

3. Naval Weapons Center. *Low Temperature Fragmentation of Mild Steel Cylinders*, by John Pearson. China Lake, Calif., NWC, March 1970. (NWC TP 4877, publication UNCLASSIFIED.)

4. John Pearson. "The Shear-Control Method of Warhead Fragmentation," in *Proceedings of the Fourth International Symposium on Ballistics*, ADPA, Monterey, Calif., 17-19 October 1978.

5. John Pearson. "The Shear-Control Fragmentation of Explosively-Loaded Cylinders," in *Metal Forming and Impact Mechanics*, ed. by S. R. Reid. London, Pergamon Press, 1985. Pp. 303-23.

6. John Pearson and S. A. Finnegan. "A Study of the Material Failure Mechanisms in the Shear-Control Process," in *Shock Waves and High Strain-Rate Phenomena in Metals*, ed. by M. A. Meyers and L. E. Murr. New York, Plenum, 1981. Pp. 205-18.

7. Naval Weapons Center. *Fragmentation Tailoring for Titanium-Case Warheads*, by John Pearson. China Lake, Calif., NWC, September 1988. (NWC TP 6947, publication UNCLASSIFIED.)

8. G. I. Taylor. "The Bursting of Cylindrical Cased Charges (1944)," in *Scientific Papers of G. I. Taylor*, Vol. 3, ed. by G. K. Batchelor. Cambridge University Press, 1963. Pp. 379-81.

9. G. I. Taylor. "The Fragmentation of Tubular Bombs (1944)," in *Scientific Papers of G. I. Taylor*, Vol. 3, ed. by G. K. Batchelor. Cambridge University Press, 1963. Pp. 387-90.

10. W. J. Stronge, Ma Xiaoqing, and Zhao Lanting. "Fragmentation of Explosively Expanded Steel Cylinders," *Int. J. Mech. Sci.*, Vol. 31, No. 11/12 (1989). Pp. 811-23.

11. Ballistics Research Laboratory. *The Initial Velocities of Fragments from Bombs, Shells and Grenades*, by R. W. Gurney. Aberdeen, Md, BRL, September 1943. (BRL report no. 405, publication UNCLASSIFIED.)

12. W. P. Walters and J. A. Zukas. *Fundamentals of Shaped Charges*. New York, John Wiley and Sons, 1989.

13. J. E. Kennedy. "Explosive Output for Driving Metal," in *Behavior and Utilization of Explosives in Engineering Design*, ed. by L. Davison, et al. Albuquerque, ASME, 1972. Pp. 109-24.

14. Naval Surface Weapons Center. *Gurney-Type Formulas for Estimating Initial Fragment Velocities for Various Warhead Geometries*, by D. K. Crabtree and S. S. Waggener. Dahlgren, Va, NSWC, June 1987. (NSWC TR 86-241, publication UNCLASSIFIED.)

15. FMC Corporation/Defense Technology Laboratories. "The Elusive $\sqrt{2E}$," by D. R. Kennedy. Santa Clara, Calif., April 1968. (Document UNCLASSIFIED.)

16. Hughes Aircraft Co.. *The Gurney Formula and Related Approximations for High-Explosive Deployment of Fragments*, by I. G. Henry. Culver City, Calif., 1967. (Report no. PUB-189, AD 813 398, publication UNCLASSIFIED.)

17. G. I. Taylor. "Analysis of the Explosion of a Long Cylindrical Bomb Detonated at One End (1941)," in *Scientific Papers of G. I. Taylor*, Vol. 3, ed. by G. K. Batchelor. Cambridge University Press, 1963. Pp. 277-86.

18. G. I. Taylor. "Blast Impulse and Fragment Velocities from Cased Charges (1943)," in *Scientific Papers of G. I. Taylor*, Vol 3, ed. by G. K. Batchelor. Cambridge University Press, 1963. Pp. 363-69.

19. G. F. Kinney and K. J. Graham. *Explosive Shocks in Air*, 2nd ed. New York, Springer-Verlag, 1985.

20. C. R. Hoggatt and R. F. Recht. "Fracture Behavior of Tubular Bombs," *J. Appl. Phys.*, Vol. 39 (1963). Pp. 1856-62.

21. S. Waggener. "The Performance of Axially Initiated Cylindrical Warheads," in *Proceedings of the Fourth International Symposium on Ballistics*. Monterey, Calif., ADPA, 17-19 October 1978.

22. Naval Weapons Center. *Engineering Elements of Explosions*, by G. F. Kinney. China Lake, Calif., NWC, November 1968. (NWC TP 4654, publication UNCLASSIFIED.)

23. P. W. Bridgman. "Fracture and Hydrostatic Pressure," in *Fracturing of Metals*. Cleveland, Am. Soc. Metals, 1948. Pp. 246-61.

24. P. W. Bridgman. *Studies in Large Plastic Flow and Fracture*. New York, McGraw-Hill, 1952.

25. J. A. Rinebolt and W. J. Harris, Jr. "Effect of Alloying Elements on Notch Toughness of Pearlitic Steels," *Trans., Am. Soc. Metals*, Vol 43, (1951). Pp. 1175-1214.

26. E. A. Parker. *Brittle Behavior of Engineering Structures*. New York, John Wiley and Sons, 1957.

27 J. S. Rinehart and John Pearson. *Behavior of Metals Under Impulsive Loads*, Cleveland, Am. Soc. Metals, 1954.

INITIAL DISTRIBUTION

20 Naval Air Systems Command
- AIR-5004 (2)
- AIR-540 (1)
- AIR-5401E1, E. Reynolds (1)
- AIR-5403 (2)
- AIR-54041 (1)
  - J. Kirkpatrick (1)
- AIR-54041C, H. Crockford (1)
- AIR-54041F, J. Smith (1)
- AIR-9301 (2)
- AIR-932 (1)
- AIR-932D (1)
- AIR-932H, Magnelli (1)
- PMA-258 (1)
- PMA-259 (1)
- PMA-268 (1)
- PMA-280 (1)
- PMA-285 (1)

5 Chief of Naval Operations
- OP-03 (2)
- OP-05 (1)
- OP-098 (1)
- OP-55 (1)

1 Director of Naval Laboratories (SPAWAR-005)
1 Chief of Naval Research, Arlington (OCNR-10P)
9 Naval Sea Systems Command
- SEA-62D (5)
- SEA-662, R. Bowen (1)
- SEA-6622, D. Porada (1)
- Technical Library (2)

1 Commander in Chief, U.S. Pacific Fleet, Pearl Harbor (Code 325)
1 Air Test and Evaluation Squadron 5, China Lake
1 Commander, Third Fleet, San Francisco
1 Commander, Seventh Fleet, San Francisco
3 David Taylor Research Center, Bethesda
- Code 1740.1, Wolk (1)
- Code 1740.2, Fisch (1)
- Code 1740.4, D. Wilson (1)

2 Naval Academy, Annapolis (Director of Research)
1 Naval Air Force, Atlantic Fleet
2 Naval Air Force, Pacific Fleet
1 Naval Air Station, North Island
2 Naval Air Test Center, Patuxent River (Central Library, Bldg. 407)
1 Naval Avionics Center, Indianapolis (Technical Library)
1 Naval Explosive Ordnance Disposal Technology Center, Indian Head
1 Naval Ocean Systems Center, San Diego (Technical Library)
1 Naval Ordnance Station, Indian Head (Technical Library)
1 Naval Postgraduate School, Monterey
1 Naval Strike Warfare Center, Fallon (Intelligence Library)
7 Naval Surface Warfare Center, Dahlgren
- G13, D. Dickinson (1)
- G22
  - Grigsby (1)
  - Swiark (1)
- G302, Dr. W. Soper (1)
- R35, Dr. B. Smith (1)
- Guided Missile Warhead Section (2)

11 Naval Surface Warfare Center, White Oak Laboratory, Silver Spring
- R04, C. Dickenson (1)
- R10, S. Jacobs (1)
- R10B, Haiss (1)
- R10C, Roslund (1)
- R12
  - J. Erkman (1)
  - Mansi (1)
  - Short (1)
- R13, R. Liddiard (1)
- R14, Kim (1)
- R15, Swisdak (1)
- Technical Library (1)

1 Naval War College, Newport
5 Naval Weapons Station, Earle, Colts Neck
- Code 8021
  - Sova (1)
  - Tetois (1)
- Code 8023
  - Bender (1)
  - Lee (1)
  - G. Miller (1)

1 Naval Weapons Station, Concord (Code 323, M. Bucher)
1 Naval Weapons Station, Yorktown (NEDED, Code 470A, Leonard)
1 Naval Weapons Support Center, Crane (Code 502)
1 Office of Naval Technology, Arlington (ONT-20)
1 Operational Test and Evaluation Force, Atlantic
3 Pacific Missile Test Center, Point Mugu
- Code 2022, Ervast (1)
- Code 2045, Torres (1)
- Technical Library (1)

1 Marine Corps Air Station, Beaufort
1 Aberdeen Proving Ground (Development and Proof Services)
2 Army Armament Research, Development and Engineering Center, Picatinny Arsenal
- SMCAR-AEE, E. Baker (1)
- SMCAR-AEM, P. Serao (1)

6 Army Ballistic Research Laboratory, Aberdeen Proving Ground
- AMXAR-SEI-B (1)
- AMXAR-T, Detonation Branch (1)
- AMXAR-TSB-S (STINFO) (1)
- AMXBR-TBD
  - Frey (1)
  - Howe (1)
  - Starkenberg (1)

1 Army Materiel Systems Analysis Activity, Aberdeen Proving Ground
2 Army Research Office, Research Triangle Park
- DRXRO-IP-L, Information Processing Office (1)
- Dr. E. Saible (1)

1 Harry Diamond Development Center, Adelphi (Technical Library)
1 Radford Army Ammunition Plant, Radford
1 Redstone Arsenal (Rocket Development Laboratory, Test and Evaluation Branch)
2 Rock Island Arsenal
- Navy Liaison Office (NVLNO) (1)
- Technical Library (SARRI-ADM-P) (1)

1 White Sands Missile Range (STEWS-AD-L)
1 Yuma Proving Grounds (STEYT-GTE, M&W Branch)

11 Air Force Munitions Systems Division, Eglin Air Force Base
AFATL/DLODL, Technical Library (1)
AFATL/FX (1)
AFATL/MNE
Aubert (1)
Corley (1)
Glenn (1)
McKenney, Jr. (1)
Parsons (1)
AFATL/MNW, J. Foster (1)
AFATL/SA (1)
MSD/SES, West (1)
MSD/XRS, J. Jenus, Jr. (1)
2 Air Force Inspection and Safety Center, Norton Air Force Base
Chief Master Sargent Speer (1)
Lt. Col. Jacobs (1)
1 Air Force Intelligence Agency, Bolling Air Force Base (AFIA/INTAW, Maj. R. Esaw)
1 Air University Library, Maxwell Air Force Base
1 Tactical Fighter Weapons Center, Nellis Air Force Base (CC/CV)
2 Wright Research and Development Center, Flight Dynamics Laboratory, Wright-Patterson Air Force Base
WRDC/FIESD
Kurtz (1)
Sparks (1)
2 57th Fighter Weapons Wing, Nellis Air Force Base
2 554th Combat Support Group, Nellis Air Force Base
OT, FWW/DTE (1)
OT, FWW/DTO (1)
1 Defense Nuclear Agency (Shock Physics Directorate)
2 Defense Technical Information Center, Alexandria
1 Department of Defense Explosive Safety Board, Alexandria (Dr. J. Ward)
1 Department of Defense-Institute for Defense Analyses Management Office (DIMO), Alexandria
1 Lawrence Livermore National Laboratory, University of California, Livermore, CA
1 Lewis Research Center (NASA), Cleveland, OH
1 Los Alamos National Laboratory, Los Alamos, NM (Reports Library)
1 California Institute of Technology, Jet Propulsion Laboratory, Pasadena, CA (Technical Library)
2 Colorado Seminary, Denver Research Institute, Denver, CO
Applied Mechanics Laboratories (1)
Technical Library (1)
2 Comarco, Incorporated, Weapon Support Division, Ridgecrest, CA
DeMarco (1)
Sewell (1)
2 Hercules Incorporated, Allegany Ballistics Laboratory, Cumberland, MD
1 Hudson Institute, Incorporated, Center for Naval Analyses, Alexandria, VA (Technical Library)
1 IIT Research Institute, Chicago, IL (Department M, Document Librarian)
3 Lockheed Missiles and Space Company, Incorporated, Sunnyvale, CA
Ordnance Systems (1)
Special Programs (1)
Tactical Support Systems (1)
1 Princeton University, Forrestal Campus Library, Princeton, NJ
1 Stanford Research Institute, Poulter Laboratories, Menlo Park, CA
4 The Johns Hopkins University, Applied Physics Laboratory, Laurel, MD
Document Library (2)
Chemical Propulsion Information Agency (2)
1 The Rand Corporation, Santa Monica, CA (Technical Library)